

1. Information on the study

| | |
|---|---|
| Data point: | KCA 7.1.2.2.1 |
| Report author | Passeport, E., et al. |
| Report year | 2014 |
| Report title | Dynamics and mitigation of six pesticides in a “Wet” forest buffer zone |
| Document No | Environmental Science and Pollution Research (2014) 21:4883–4894 |
| Guidelines followed in study | None |
| Deviations from current test guideline | None |
| GLP/Officially recognised testing facilities | No, not conducted under GLP/Officially recognised testing facilities |
| Acceptability/Reliability: | Reliable with restrictions (Not all parameters are reported to check validity of the study) |

2. Full summary of the study according to OECD format

Pesticide pollution is one of the main current threats on water quality. This paper presents the potential and functioning principles of a “Wet” forest buffer zone for reducing concentrations and loads of glyphosate, isoproturon, metazachlor, azoxystrobin, epoxiconazole, and cyproconazole. A tracer injection experiment was conducted in the field in a forest buffer zone at Bray (France). A fine time-scale sampling enabled to illustrate that interactions between pesticides and forest buffer substrates (soil and organic rich litter layer), had a retarding effect on molecule transfer. Low concentrations were observed for all pesticides at the forest buffer outlet thus demonstrating the efficiency of “Wet” forest buffer zone for pesticide dissipation. Pesticide masses injected in the forest buffer inlet directly determined concentration peaks observed at the outlet. Rapid and partially reversible adsorption was likely the major process affecting pesticide transfer for short retention times (a few hours to a few days). Remobilization of metazachlor, isoproturon, desmethylisoproturon, and AMPA was observed when non-contaminated water flows passed through the forest buffer. Our data suggest that pesticide sorption properties alone could not explain the complex reaction mechanisms that affected pesticide transfer in the forest buffer. Nevertheless, the thick layer of organic matter litter on the top of the forest soil was a key parameter, which enhanced partially reversible sorption of pesticide, thus retarded their transfer, decreased concentration peaks, and likely increased degradation of the pesticides. Consequently, to limit pesticide pollution transported by surface water, the use of already existing forest areas as buffer zones should be equally considered as the most commonly implemented grass buffer strips.

Materials and Methods

The forest buffer zone is located at the outlet of a tile drained agricultural watershed at Bray (France).

Chemicals

An injection solution was prepared with six pesticides and potassium bromide as a conservative tracer. Pesticides were provided by farmers and diluted in deionized water before injection. Commercial solutions that were used are indicated into parentheses: three herbicides, glyphosate (Glyphogan), isoproturon (Isoproturon), and metazachlor (Novall), and three fungicides, azoxystrobin (Priori Xtra), cyproconazole (Amistar Xtra), and epoxiconazole (Opus) were selected for their contrasting properties and wide use in agriculture.

Tracer Experiment

The forest buffer tracer experiment took place for a period of 14 days, from 19 February 2009, 10:50 to 5 March 2009, 13:20 in a reduced portion of the forest buffer, using watershed outlet flows as incoming flows into the forest buffer. The experimental plot was delimited with soil border levees leading to a 54 m² surface area (36 m×1.5 m). Only one significant rainfall event occurred on 308.5 h after the start

of the experiment, with a cumulative rainfall depth of 9.94 mm, measured with the on-site tipping bucket rain gauge (R01 3030A Danae, Précis Mécanique, Bezons, France). Water temperature was 5.9 ± 3.7 °C during the course of the experiment, and was close to or greater than monthly averages. The inlet flow rate was 0.32 ± 0.08 L/s. At the outlet, a flow restriction helped manually measuring flow rates by frequently timing the filling of a container with a known volume. Water from the watershed was allowed to flow through the forest buffer experimental plot on 18 February 2009 at 15:50, in order to saturate the soil and ensure a permanent flow rate for the next day injection. Two peristaltic pumps (Eijkelkamp 12 V SDEC Reignac-sur-Indre, France) were used to ensure a 0.30 L/s injection flow rate during 78 s. Grab water samples or samples collected by means of a time-dependent automated sampler (ISCO 3700 Neotek, Trappes, France) were taken at the outlet of the experimental plot. The sampling frequency was modified along the course of the experiment: every 15 min for the first 7 h, every 30 min until 28.5 h after the start of the experiment, then every 3 h until 94 h since injection, and every 10 h from days 4 to 10 following the start of the experiment. Finally, five grab water samples were taken at forest buffer inlet to control pesticides' background concentrations coming from the artificially drained watershed.

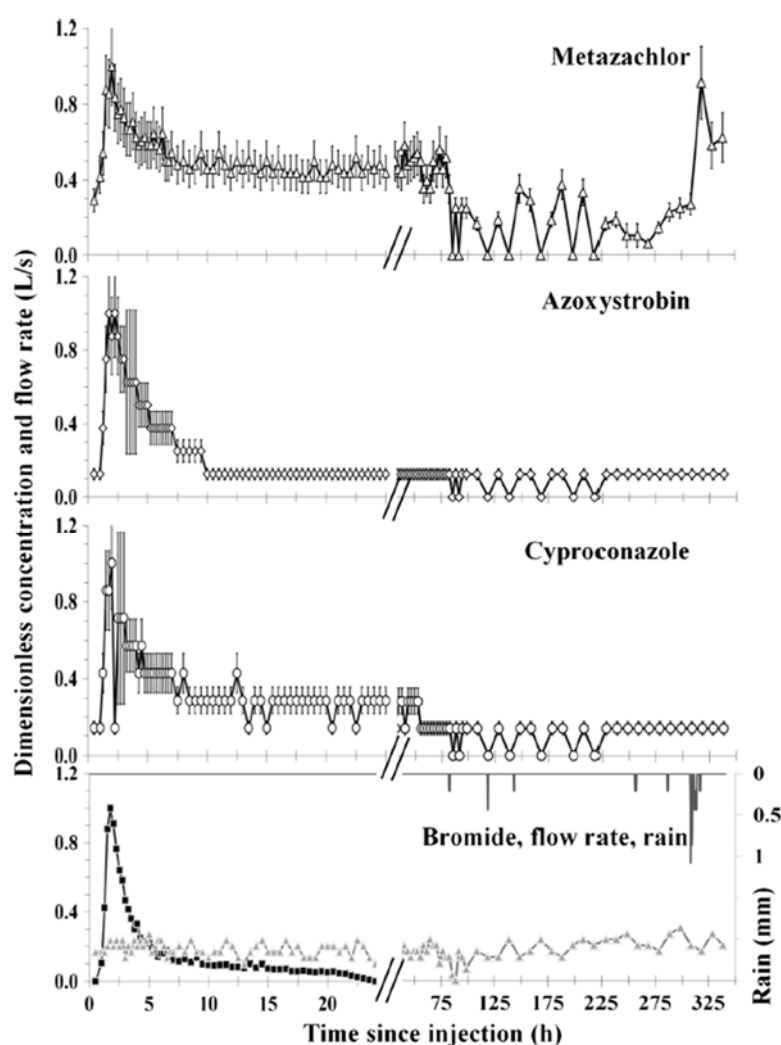


Figure 1. Flowrate at the forest outlet (gray triangle, bottom panel, in liter per second), and dimensionless (C/C_{\max}) concentration pattern during the first 24 h (left panels) and the next 350 h (right panels) after injection, for molecules that exhibited the clearest transfer pattern: metazachlor (white triangles), azoxystrobin (white diamonds), cyproconazole (white circles), and bromide (black squares). The double slash bars (//) indicate a change in time step. C concentration at time t ; C_{\max} peak concentration measured 2 h (metazachlor, azoxystrobin, and cyproconazole) and 1.8 h (bromide) after injection. No rainfall event occurred during the first 24 h; rain beyond 24 h (bottom-most right-hand side panel) is plotted on the right hand vertical axis, in reverse order. Error bars correspond to dimensionless expanded uncertainties, i.e., expanded uncertainties on concentrations (U , coverage factor = 2), divided by C_{\max}

Analytical method

Water sample analysis

Subsamples were taken from water samples, filtered and analyzed for bromide with ion chromatography and an IonPac AS9-HC column. The limit of quantification (LQ) was 1 mg/L. Metazachlor, cyproconazole, epoxiconazole, azoxystrobin, isoproturon and two of its metabolites, desmethyisoproturon and 1-(4-isopropylphenyl)urea, were extracted by solid-phase extraction on pre-filtered samples, and then analyzed by high-performance liquid chromatography coupled with triple quadrupole mass spectrometry (LCMS-MS). Limits of quantification were 0.02 µg/L for these seven pesticides and metabolites. Glyphosate and its main metabolite, AMPA, were first derivatized with 9-fluorenylmethyl chloroformate (FMOC) before LC-MS-MS analysis (LQ=0.1 µg/L for both glyphosate and AMPA).

Litter and soil sampling and analysis

Litter, and soil grab samples were taken in the forest experimental plot at the end of the tracer experiment. Another litter and soil samples were collected outside the experimental plot to compare with those collected inside the experimental plot. All samples were frozen before pesticide analysis. Glyphosate and AMPA were extracted by ultrasonic waves in water, then derivatized with FMOC and analyzed by LCMS-MS, whereas extraction for the other molecules from soil samples was carried out with ultrasonic waves in acetone. Extracts were analyzed by LC-MS-MS. Litter samples were treated with an internal procedure developed by the laboratory (Institut Pasteur de Lille). Limits of quantification were 0.01 mg/kg dry weight for each compound.

Data analysis

The hydraulic retention time was calculated based on the bromide conservative tracer using the moment theory on residence time distribution (see Passeport et al. (2010), Kadlec and Wallace (2008)).

Statistical analyses

Pearson correlation coefficients were determined with the R software to detect possible correlations among pesticide concentrations, injected masses, and pesticide physico-chemical properties.

Table 1. Forest buffer inlet concentrations

| Molecule | Pesticide inlet concentrations (µg/L) | | | | |
|---------------------------|---------------------------------------|-------------------|------|-------|------|
| | Time from injection (h) | | | | |
| | LQ ^a | -0.58 | 6.75 | 24.17 | 339 |
| Glyphosate | 0.1 | n.d. ^b | <LQ | <LQ | n.d. |
| AMPA | 0.1 | 0.30 | <LQ | <LQ | 0.30 |
| Isoproturon | 0.02 | 1.60 | 1.20 | 1.30 | 1.40 |
| Desmethyisoproturon | 0.02 | 0.12 | 0.11 | 0.10 | 0.11 |
| 1-(4-isopropylphenyl)urea | 0.02 | <LQ | <LQ | <LQ | n.d. |
| Metazachlor | 0.02 | 0.29 | 0.30 | 0.25 | 0.19 |
| Epoxiconazole | 0.02 | <LQ | 0.02 | n.d. | n.d. |
| Azoxystrobin | 0.02 | <LQ | <LQ | n.d. | n.d. |
| Cyproconazole | 0.02 | <LQ | <LQ | n.d. | n.d. |

^a Limit of quantification

^b n.d. is "not detected"

Results

Hydrology

Water ran off through the forest buffer experimental plot as a shallow sheet flow with an average outlet flow rate of 0.18± 0.11 L/s (average ± expanded uncertainty for 95 % confidence interval). Bromide

started to be detected 1 h after injection and reached a concentration peak 1.8 h after injection (Fig. 1). Bromide recovery rate and hydraulic residence time were 74 % and 6.3 h, respectively.

Inlet water quality

During the experiment, watershed tile-drain flows continuously entered the experimental plot at a controlled flow rate of 0.3 L/s. We determined that some of the studied pesticides also entered the experimental plot via watershed flows during the course of the experiment. Non-negligible concentrations of isoproturon, desmethylisoproturon, glyphosate, AMPA and metazachlor were measured (Table 1). Epoxiconazole was detected once (6.8 h after injection) but with a concentration at the limit of quantification. The most recent applications of glyphosate and metazachlor on the Bray watershed were approximately 16 months before the start of the experiment.

Table 2. Tracer experiment dynamics characteristics and mass recovery rates

| Molecule | Peak conc \pm U(C) ($\mu\text{g/L}$) | Peak conc time (h after injection) | Percent recovery (%) | Time for conc reaching < LQ (h after injection) |
|---------------------------|---|---------------------------------------|-------------------------|--|
| Bromide | 1750 | 1.75 | 74 | 24.0 |
| Glyphosate | 0.05 ± 0.03 | NA ^a | NA | NA |
| AMPA | 0.30 ± 0.08 | 1.75 | NA | NA |
| Isoproturon | 1.70 ± 0.41 | 2.50 | NA | NA |
| Desmethylisoproturon | 0.14 ± 0.03 | NA | NA | NA |
| 1-(4-isopropylphenyl)urea | 0.02 ± 0.01 | NA | NA | NA |
| Metazachlor | 0.48 ± 0.10 | 2.00 | NA | NA |
| Epoxiconazole | 0.04 ± 0.01 | 2.75 | NA | NA |
| Azoxystrobin | 0.08 ± 0.02 | 2.00 | 22 | 10.0 |
| Cyproconazole | 0.07 ± 0.02 | 2.00 | 45 | 13.5 |

^aNA means Not Available, when peak concentration ("Peak Conc") time could not be clearly identified and mass balances could not be reasonably calculated due to a large portion of the concentration dataset below limits of quantifications

Pesticide dynamics description

Table 2 presents the main characteristics for pesticide concentration peaks, dynamics and mass balances. Apart from isoproturon, concentrations were lower than 0.50 $\mu\text{g/L}$ for AMPA and metazachlor, and did not exceed 0.15 $\mu\text{g/L}$ for the other pesticides (glyphosate, azoxystrobin, epoxiconazole, cyproconazole, desmethylisoproturon, and 1-(4-isopropylphenyl)urea). Only injections of metazachlor, azoxystrobin and cyproconazole resulted in a clear transfer pattern at the forest plot outlet (Fig. 1). Two hours after injection, these pesticides exhibited concentration peaks of 0.48 ± 0.10 , 0.08 ± 0.02 , and 0.07 ± 0.02 $\mu\text{g/L}$ for metazachlor, azoxystrobin, and cyproconazole, respectively. These concentration peaks were observed closely after that of the conservative tracer, which was recorded 1.8 h after injection (Table 2). For glyphosate, AMPA, epoxiconazole, and 1-(4-isopropylphenyl)urea, concentrations at the forest plot outlet were so low that only a qualitative assessment of the data can reasonably be performed. In addition, high background concentration levels of isoproturon and desmethylisoproturon hindered an accurate quantitative analysis of the data for these two molecules. In all water samples, glyphosate concentrations were below the LQ and those for AMPA never exceeded 0.30 ± 0.08 $\mu\text{g/L}$. No temporal variation was observed for these molecules, besides two small AMPA concentration rises, one after injection (between 1.8 and 3.8 h) and a second one after the rainfall event (between 318.5 and 328.5 h). Concentration peaks for the injected molecules were significantly correlated (p value= 1.75×10^{-5}) with background concentrations, highlighting the strong influence that this artifact exerted on the results. The second strongest correlation (despite not significant at a $\alpha=5$ % significance level) was between pesticide concentration peaks and injected masses. With this small dataset, no statistically significant correlations were found between the ratios and the pesticide sorption properties.

Discussion

Hydrology

The ratio between outlet and inlet flow rates (0.61), and the bromide recovery rate (74 %) are suggestive of some water losses outside the experimental plot, via infiltration, possibly due to poor soil levee compaction, earthworm burrows, and tree roots.

Forest buffer efficiency for pesticide removal

A key conclusion of our study relies on the fact that, for most pesticides, very low concentrations were measured at the forest outlet, thus demonstrating the efficiency of such buffer zones for pesticide removal.

Sorption as part of a complex set of removal processes

The high sorption coefficients of glyphosate, AMPA and epoxiconazole may partly explain their low concentrations measured at the forest outlet. Contrary to glyphosate and AMPA, epoxiconazole was detected on dead leaves at the forest plot inlet and middle zones 14 days after injection even after large rainfall events. This supports a possible strong adsorption of epoxiconazole onto the forest litter. Because epoxiconazole was not detected in the soil below the litter layer, it is likely that the litter layer acted as a key sorption material that prevents strongly sorbing pesticides from leaching to deep soil horizons.

Degradation and remobilization of pesticides

Due to the moderately long half-lives of their parent molecules, glyphosate and isoproturon, the detection of AMPA and desmethylisoproturon at the beginning of the experiment can hardly be attributed to the injected parent molecules. It should be noted that AMPA, isoproturon, and desmethylisoproturon were detected at the forest plot inlet indicating that these molecules were also transferred to the experimental plot from the tile-drain watershed. Glyphosate and isoproturon were applied previously on the agricultural watershed and may have been partially degraded in the catchment and forest buffer soils thus generating these metabolites.

“Dry” vs. “Wet” buffer zone

In this study, the “Wet” forest buffer soil had a high clay content thus limiting downward infiltration. Even if water losses via infiltration might occur, it could not explain alone the observed pesticide removal. It is a fundamental difference with “Dry” buffer zones like grass areas, where infiltration plays a crucial role. The second major difference between grass and forest buffer zones lies in the presence of thick litter layer rich in organic matter in the latter. The litter provides many sorption sites for pesticides and is biologically active, thereby biodegrading retained pesticides. Consequently, when buffer zone soil is saturated, pesticide sorption and degradation should more easily occur in forested areas than in grass areas, provided that the contaminated water runs off through the litter layer as a shallow and slow water flow.

Conclusions

The objective of this experiment was to demonstrate at the field scale the potential of forest buffer zones to reduce the concentrations and loads of pesticides presenting a wide range of physico-chemical properties. Very low concentrations were measured at the forest outlet thus suggesting a potential of the forest buffer to effectively reduce the pollution with pesticides. Understanding processes, which govern the removal of pesticides through the forest buffer was beyond the scope of this study. However, the fine sampling frequency used in this study helped to provide some explanations about the observed dynamics of pesticide transfer through the forest buffer zone. At short time-scales (lower than a month), retention processes are suspected to dominate. Our results highlighted the dual role of organic matter. On the one hand, organic substrates enabled rapid adsorption of pesticides transported in highly contaminated flows. On the other hand, when fresher (i.e., less contaminated) flows crossed the forest buffer, previously adsorbed pesticides were shown to desorb thus being released back to the water column. Organic matter also plays an indirect role in this process as it supports growth of microbial populations. Any forested area adequately located in the landscape could be used as an efficient buffer zone for reducing pesticide pollution. Indeed, even old wood that were not necessarily well maintained could be good candidates for buffering pesticide contaminated flows provided a thick litter layer has

had time to accumulate over time. At a short time scale (here approx. 350 h), highly organic material would therefore mainly act as a retarding factor that temporarily affect pesticide dynamics. For extended periods of water retention, degradation reactions leading to metabolites are likely to occur, however, more research is needed to confirm the extent of pesticide degradation that could be achieved. The results of this study are suggestive of a high potential of “Wet” forest buffer zone for the reduction of downstream pesticide concentrations and loads. Further research should investigate the efficiency of forest buffers for pesticide removal (1) under various climatic conditions, and for a wide range of forest buffer (2) sizes and shapes, and (3) locations in the watershed (headstream vs. downstream). Such results are needed to better understand pesticide fate and the role of the litter layer, and to establish guidelines to design forest buffer zones and incorporate them in land management strategies.

3. Assessment and conclusion

Assessment and conclusion by applicant:

The study describes the mitigation of glyphosate among other pesticides by a wet forest buffer zone in France. Not all required parameters are reported to check validity of the study (e.g. information on test substance, analytical method, characterization of soil).

The study is classified reliable with restrictions (Category 2).

1. Information on the study

| | |
|---|--|
| Data point: | KCA 7.1.3.1.1 |
| Report author | Rampoldi, E., et al. |
| Report year | 2014 |
| Report title | Carbon-14-Glyphosate Behavior in Relationship to Pedoclimatic Conditions and Crop Sequence |
| Document No | Journal of Environmental Quality 43:558–567 (2014) |
| Guidelines followed in study | None |
| Deviations from current test guideline | None |
| GLP/Officially recognised testing facilities | No, not conducted under GLP/Officially recognised testing facilities |
| Acceptability/Reliability: | Reliable with restrictions (No EU conditions, missing information for validity check) |

2. Full summary of the study according to OECD format

The recognition of glyphosate [(N-phosphonomethyl) glycine] behavioral patterns can be readily examined using a pedoclimatic gradient. In the present study, glyphosate adsorption–desorption and degradation were examined under different scenarios in relationship to soil properties and soil use applications. Three sites with varied pedoclimatic conditions and two crop sequences were selected. Adsorption–desorption and glyphosate distribution in mineralized, extractable, and non-extractable fractions were assessed under laboratory conditions. Glyphosate sorption was characterized by isotherms and glyphosate degradation using the distribution of ^{14}C -glyphosate radioactivity among mineralized fractions, two extractable fractions (in water, ER1; in NH_4OH , ER2), and non-extractable fractions. Results showed sorption indices (distribution coefficient K_d and Freundlich sorption coefficient K_f : 13.4 ± 0.3 – 64.1 ± 0.9 L/kg and 16.2–60.6, respectively), and hysteresis increased among soil sites associated with decreasing soil particle size <2 μm , soil organic matter, and other soil properties associated with soil granulometry. A multiple stepwise regression analysis was applied to estimate the relationship between K_d values and soil properties. Cation exchange capacity, water field capacity, and Bray-1 P were the soil properties retained in the equation. Soils under continuous soybean [*Glycine max* (L.) Merr.] (monoculture) treatment exhibited reduced glyphosate adsorption and decreased hysteresis desorption relative to soils under rotation. To our knowledge, these results are the first to demonstrate that soils with identical properties exhibited different glyphosate retention capacities based on crop sequence. We propose possible explanations for this observation. Our results suggested that characterization of the variability in soil property gradients can serve to determine glyphosate behavioral patterns, which can establish a criterion for use in reducing potential environmental risks.

Materials and Methods

Soils

The province of Cordoba, Argentina, is characterized by broken relief to the west and plains in the central and eastern parts. The dominant parent materials are sediments transported by wind, called *loess*, from the mountain range of Los Andes. Three sites were selected: Pampa de Pocho (PP), Manfredi (M), and Marcos Juarez (MJ). At each site, two crop sequences were investigated, a monoculture of soybean with four glyphosate applications of 6 L/ha (2880 g a.i./ha) during the year and a soybean–maize rotation with only one glyphosate application of 2 L/ha (960 g a.i./ha). The soil was sampled at 0–5 cm. All samples were characterized by particle size determined by sedimentation, water-holding capacity (WHC) by membrane pressure plate, and the permanent wilting point (PWP) by ceramic pressure plate. Soil pH in water (soil/water, 1:1), and total organic C content (TOC) by wet combustion, extractable P by Bray 1, cation-exchange capacity (CEC) by NH_4OAc saturation, exchangeable Ca^{2+} and Mg^{2+} by complexometric titration with ethylenediaminetetraacetic acid, and exchangeable Na^+ and K^+ by flame photometer.

Table 1

Main characteristics of the three soils under two cropping sequences, a soybean monoculture and a soybean–maize rotation.

| Property | Marcos Juárez | | Manfredi | | Pampa de Pocho | |
|---|-----------------|------------|------------------|------------|------------------|------------|
| Altitude, m asl | 110 | | 292 | | 1026 | |
| Annual avg. temperature, °C | 17.9 | | 16.8 | | 16.6 | |
| Mean annual precipitation, mm | 931 | | 787 | | 523 | |
| Soil type | Typic Argiudoll | | Typic Haplustoll | | Entic Haplustoll | |
| Main textural class† | clay loam | | loam | | sandy loam | |
| | Monoculture | Rotation | Monoculture | Rotation | Monoculture | Rotation |
| pH | 5.2 ± 0.1 | 5.5 ± 0.2 | 6.1 ± 0.1 | 6.3 ± 0.1 | 6.7 ± 0.1 | 6.2 ± 0.1 |
| Water holding capacity, g kg ⁻¹ | 300 | 280 | 220 | 250 | 80 | 150 |
| Permanent wilting point, g kg ⁻¹ | 130 | 130 | 100 | 100 | 40 | 70 |
| Clay, g kg ⁻¹ | 278 ± 2 | 242 ± 18 | 200 ± 4 | 216 ± 18 | 146 ± 15 | 170 ± 8 |
| Silt, g kg ⁻¹ | 580 ± 9 | 602 ± 15 | 558 ± 20 | 520 ± 20 | 88 ± 11 | 268 ± 21 |
| Sand, g kg ⁻¹ | 142 ± 7 | 156 ± 3 | 242 ± 5 | 264 ± 5 | 766 ± 22 | 562 ± 15 |
| Total organic C, g kg ⁻¹ | 17.2 ± 0.9 | 17.0 ± 0.1 | 14.3 ± 0.27 | 15.8 ± 0.5 | 7.3 ± 0.9 | 9.9 ± 0.3 |
| Bray-1 P, mg kg ⁻¹ | 58.0 ± 1.0 | 57.0 ± 1.0 | 53.0 ± 1.0 | 55.0 ± 1.0 | 12.0 ± 0.3 | 45.0 ± 1.0 |
| Cation exchange capacity, cmol kg ⁻¹ | 19.6 ± 0.1 | 18.8 ± 0.2 | 18.9 ± 0.1 | 19.0 ± 0.1 | 15.0 ± 0.1 | 9.0 ± 0.1 |
| Ca, cmol kg ⁻¹ | 11.8 ± 0.1 | 10.9 ± 0.1 | 12.1 ± 0.1 | 12.1 ± 0.1 | 9.4 ± 0.1 | 6.3 ± 0.1 |
| Mg, cmol kg ⁻¹ | 3.2 ± 0.1 | 3.4 ± 0.1 | 3.7 ± 0.1 | 3.6 ± 0.1 | 3.0 ± 0.1 | 1.5 ± 0.1 |
| K, cmol kg ⁻¹ | 2.3 ± 0.1 | 2.5 ± 0.1 | 2.8 ± 0.1 | 2.8 ± 0.1 | 2.2 ± 0.1 | 0.7 ± 0.1 |
| Na, cmol kg ⁻¹ | 0.3 ± 0.1 | 0.3 ± 0.1 | 0.2 ± 0.1 | 0.2 ± 0.1 | 0.2 ± 0.1 | 0.2 ± 0.1 |

Soil size fractionation was done by dispersion of soils in water. The fractions 2000 to 200, 200 to 50, and <50 µm were recovered from the dispersed suspension by sieving and dried at 50°C. The soil weight and organic C concentration in each fraction were quantified.

Carbon-14-Glyphosate Retention

A solution of [methyl-¹⁴C]glyphosate was purchased from Sigma Chemical Co. (81 MBq/mmol, 99.2% radiopurity) and was prepared in Milli-Q water by isotopic dilution with unlabeled glyphosate (>99% purity) at six different concentrations (0.2, 0.5, 1, 2, 5, and 10 mg/L). Each solution contained 0.166 MBq/L. Two-gram subsamples of air-dried soil were placed in 25-mL Corex glass centrifuge tubes and 10 mL of ¹⁴C-glyphosate solution at one of the six different concentrations was added. Blanks without soil were included and each soil and glyphosate concentration combination was prepared in triplicate. The tubes were shaken by rotation for 24 h at 20 ± 2°C in the darkness. After shaking, the tubes were centrifuged for 15 min at 1800 x g and supernatant removed. The ¹⁴C-glyphosate concentrations in the supernatant solution were calculated with a Packard Tri-Carb 2100 TR liquid scintillation counter (Packard Instruments) from the supernatant radioactivity measurements. The amount of sorbed glyphosate per mass of soil was calculated from the difference in herbicide concentration before and after sorption. Desorption of ¹⁴C-glyphosate was studied in all samples initially treated with 10 mg glyphosate/L during the adsorption study. After sorption equilibration, most of the supernatant was removed and replaced by an equivalent volume of Milli-Q water. The tubes were vortexed to disperse the soil pellets, and the suspensions were mechanically shaken for 24 h at 20 ± 2°C. The suspensions were then centrifuged for 15 min at 1899 x g, and the supernatant was again replaced with Milli-Q water. Five successive desorption treatments were done for each sample. The supernatant radioactivity was determined after each desorption to quantify the amount of desorbed herbicide.

Table 2Freundlich sorption–desorption isotherm parameters (adsorption $K_{f,ads}$ and n_{ads} , desorption $K_{f,des}$ and n_{des} , and hysteretic index H) and distribution coefficients (K_d) of glyphosate in three soils under two cropping sequences.

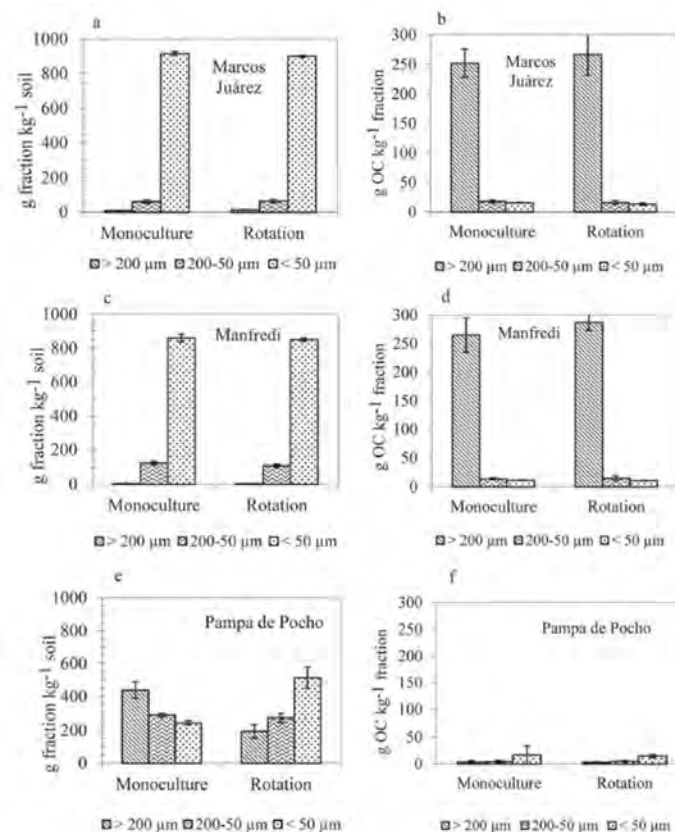
| Location | Cropping sequence | Sorption | | | | | Desorption | | | <i>H</i> |
|----------------|-------------------|---------------------------|-------------------------|-----------------------|-----------------------|-----------------------|---------------------------|-------------------------|-----------------------|-------------|
| | | <i>K</i> _{f,ads} | <i>n</i> _{ads} | <i>R</i> ² | <i>K</i> _d | <i>R</i> ² | <i>K</i> _{f,des} | <i>n</i> _{des} | <i>R</i> ² | |
| | | L kg ⁻¹ | | | | | | | | |
| Marcos Juárez | monoculture | 48.8 ± 0.3 | 0.91 ± 0.01 | 0.99 | 50.1 ± 0.5 | 0.98 | 44.9 ± 0.6 | 0.17 ± 0.01 | 0.90 | 0.19 ± 0.02 |
| | rotation | 60.6 ± 0.8 | 0.90 ± 0.02 | 0.99 | 64.1 ± 0.9 | 0.95 | 45.2 ± 0.5 | 0.11 ± 0.01 | 0.93 | 0.12 ± 0.03 |
| Manfredi | monoculture | 29.3 ± 0.1 | 0.84 ± 0.01 | 0.99 | 28.4 ± 0.5 | 0.97 | 36.3 ± 0.3 | 0.23 ± 0.01 | 0.95 | 0.27 ± 0.02 |
| | rotation | 42.6 ± 0.4 | 0.86 ± 0.02 | 0.99 | 43.7 ± 0.7 | 0.88 | 43.1 ± 0.5 | 0.16 ± 0.01 | 0.85 | 0.19 ± 0.03 |
| Pampa de Pocho | monoculture | 16.2 ± 0.2 | 0.77 ± 0.01 | 0.99 | 13.4 ± 0.3 | 0.96 | 24.7 ± 0.3 | 0.30 ± 0.02 | 0.90 | 0.39 ± 0.03 |
| | rotation | 20.3 ± 0.1 | 0.85 ± 0.01 | 0.99 | 18.7 ± 0.3 | 0.98 | 26.5 ± 0.3 | 0.16 ± 0.01 | 0.87 | 0.19 ± 0.02 |

Carbon-14-Glyphosate Behavior

The mineralization of ^{14}C -glyphosate was followed during laboratory incubations (in triplicate) of 49 d at $28 \pm 1^\circ\text{C}$ in the dark. One milliliter of the ^{14}C -glyphosate solution was added to 10 g of each soil. The soil water content was adjusted to 85% of WHC of each soil with Milli-Q water, taking into account the glyphosate solution. The ^{14}C - CO_2 evolved during the incubation was trapped in NaOH. The vials containing NaOH were sampled and replaced after 3, 7, 14, 21, 28, 35, 42, and 49 d. The total radioactivity content was measured by liquid scintillation counting using a Tri-Carb 2100 TR counter and with external standardization and Ultima Gold XR as a scintillation cocktail.

Extractable and Non-extractable Residues

At the 49th d of the incubation period, four sequential extractions were done for the corresponding soil samples. The extractable fraction of ^{14}C -glyphosate was obtained in two steps. The first extraction was done using 50 mL of Milli-Q water during 24 h, the supernatant was recovered, and the radioactivity was measured by scintillation counting (ER1). After that, three successive extractions were performed, each 24, 24, and 4 h, respectively, with 50 mL of 0.5 mol/L NH_4OH in glass centrifuge tubes. The three successive extracts were pooled for each soil sample and the radioactivity was measured by scintillation counting (ER2). Radioactivity in the solid soil samples containing non-extractable ^{14}C -glyphosate residues (NER) were recovered and dried at 40°C . The radioactivity was measured on three subsamples (100–200 mg) by scintillation counting after combustion at 800°C under O_2 flow in a sampler oxidizer (Packard) followed by ^{14}C - CO_2 trapping in 8 mL of Carbosorb E (Packard) mixed with 12 mL of Permafluor E+ (Packard).



Distribution of soil mass and organic C (OC) content in three soil size fractions (2000–200, 200–50, and <50 μm) in three soils and two cropping sequences.

Figure 1

Mathematical Adjustment and Statistical Analysis

Sorption Isotherms

The amounts of ^{14}C -glyphosate adsorbed on the soil (x/m, mg glyphosate/kg solid) were calculated as the difference between the initial ^{14}C -glyphosate concentration and the supernatant concentration (C, mg glyphosate/L supernatant solution). Glyphosate sorption isotherms were described by the Freundlich model and the linear model.

Kinetics of Degradation

Cumulative ^{14}C -CO₂ glyphosate and C-CO₂ evolved were adjusted to a first-order model:

Statistical Analysis

An ANOVA procedure was performed using the soil type (location) as the main factor, with six replicates per soil. Fisher's test of comparison of means was used. Multiple regression analysis was also performed between glyphosate K_d values and soil properties: sand, clay, silt, pH, TOC, CEC, Ca²⁺, Mg²⁺, Na⁺, K⁺, WHC, PWP, Bray-1 P, and three organic C fractions (>200, 50–200, and <50 μm). The criteria for the selection of the variables were $p < 0.05$. For each crop sequence (monoculture or rotation), a simple ANOVA by each soil with three replicates was used. The statistics software used was Infostat (Di Rienzo et al., 2009).

Table 3

Stepwise linear regression of glyphosate sorption index K_d .

| Variable | Coefficient | SE | P | R^2 | Adjusted R^2 |
|--------------------------|-------------|-------|--------|-------|----------------|
| | −48.04 | 13.22 | 0.0027 | | |
| Water field capacity | 130.68 | 29.6 | 0.0006 | | |
| Bray-1 P | −0.54 | 0.14 | 0.0018 | | |
| Cation exchange capacity | 3.53 | 1.4 | 0.0243 | | |
| | | | | 0.97 | 0.96 |

Results and Discussion

Soil Characterization

Edaphoclimatic characteristics from each of the three scenarios studied are shown in Table 1. The PP soils positioned at the northwestern sampling site exhibited a sandy texture, the highest pH and the lowest TOC, CEC, PWP, and WHC. At the extreme southeastern sampling site, the MJ soils showed the lowest pH and the highest TOC, CEC, PWP, WHC, and clay and silt contents. The M soils located in the geographically intermediate sampling site also exhibited intermediate edaphic properties in relationship to the other two sampling sites.

The soil size distribution among fractions ranged from 2000 to 200, 200 to 50, and <50 μm (Fig. 1a, 1c, 1e) and showed granulometric differences among the three sample sites. The M and MJ sites primarily differed in the fraction proportion in micrometers (i.e., 200–50), corresponding to the categories of fine sand and very fine sand. The PP soils differed from the other two sampling sites in the proportion and distribution of the three soil size categories evaluated. Rotation and monoculture treatments revealed identical soil size distributions for M and MJ. However, the two cropping sequence treatments from the PP site were not congruent with M and MJ, and significant differences in soil particle size distribution were observed ($P < 0.05$). Results showed that the coarsest soil size fraction (2000–200 μm) containing fresh soil organic matter (SOM) represented the largest organic C concentration in MJ and M soils and both treatments (monoculture and rotation) (Fig. 1b and 1d). Nevertheless, the highest TOC proportion corresponded to humified organic matter associated with a soil size fraction <50 μm , i.e., the highest proportion of this fraction was present in these soils (between 75 and 85%). Carbon enrichment in some of the three soil size fractions, which was associated with soil texture and granulometry, was not found in the PP soils (Fig. 1f).

Carbon-14-Glyphosate Sorption–Desorption

Carbon-14-glyphosate sorption-desorption isotherms obtained from the three scenarios evaluated are shown in Fig. 2. The experimental data were fitted with two mathematical models: the Freundlich adsorption isotherm and the linear model. Empirical evidence indicated that as the value of n_{ads} decreased,

the linear approximation became less satisfactory, especially at high and low concentrations, and discrepancies between K_f and K_d values occurred. Our results showed that the equilibrium concentration range was 0.1 to 1.0 mg/L (MJ soils), 0.1 to 1.5 mg/L (M soils), and 0.1 to 3 mg/L (PP soils), and $K_{f,ads}/K_d$ ranged between 0.9 and 1.1.

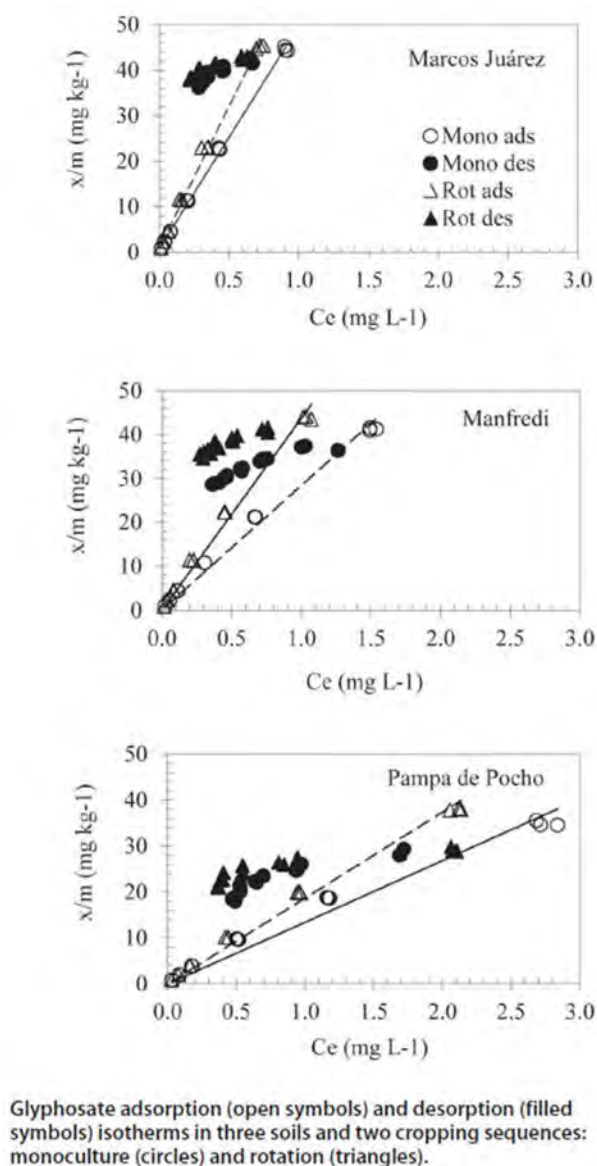


Figure 2

The three scenarios examined clearly differed in glyphosate adsorption. The $K_{f,ads}$ and K_d indices showed a threefold increase from PP soils (northwest position) to MJ soils (southeast position). Our results from the three sampling sites showed a geographic gradation in soil characteristics that were associated with glyphosate adsorption, i.e., we detected a relation among geographic position, edaphic characteristics, and glyphosate adsorption capacity. That behavioral pattern was confirmed by adsorption studies. The PP site collective soil characteristics were associated with low glyphosate adsorption capacity, i.e., high pH, low clay content and SOM, while the MJ site exhibited inverse soil attributes and an overall high adsorption capacity. A multiple linear regression analysis was performed to estimate the relationship between glyphosate K_d values and soil properties (Table 3). The PWP, CEC, and Bray-1 P were the regressed variables retained in the analysis, which explained 93% ($R^2 = 0.97$) of the total variation. Desorption isotherms were fitted for the Freundlich model. An irreversible desorption process was shown by the lack of overlap in the sorption - desorption isotherms (Fig. 2). Glyphosate desorption indices were higher than corresponding adsorption indices. Our study revealed that glyphosate

desorption hysteresis increased from the northwest toward the southeast sampling sites. The H indices, which ranged from 0.12 to 0.39, were used to compare the hysteresis degree among soils. Between 15 and 57% of the glyphosate initially applied was desorbed. The PP soils exhibited the highest ^{14}C -glyphosate desorption, with >50% recovered in the first desorption step. On the contrary, for the M and MJ soils in the first desorption step, only about 30% of the total ^{14}C -glyphosate was desorbed. Crop sequence effects were evaluated only for the M and MJ soils. These two sample sites had similar soil characteristics, while the PP site differed and was therefore excluded. The extent of glyphosate adsorption and desorption hysteresis was higher in rotation than monoculture soils (Fig. 3; Table 2). To our knowledge, our results are the first to document that soils with identical properties exhibited different glyphosate retention capacities due to cropping sequence.

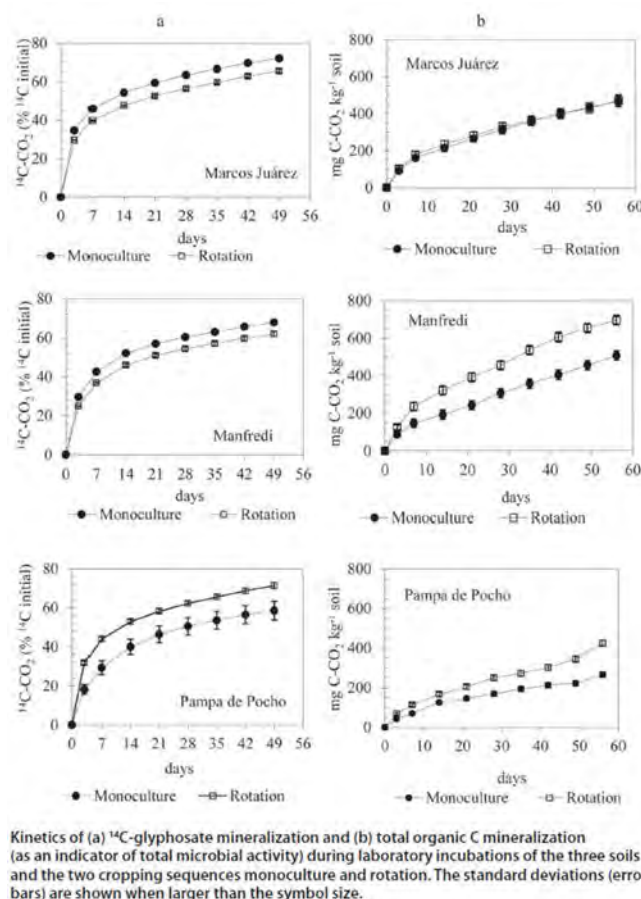


Figure 3

Carbon-14-Glyphosate Mineralization

Carbon-14-glyphosate mineralization kinetics together with C-CO_2 evolution are shown in Fig. 3. In addition, cumulative glyphosate mineralization and oxidizable C after 49 d of incubation are shown in Table 4. At the end of the incubation period, the $^{14}\text{C}\text{-CO}_2$ released ranged from 61.7 to 72.8% of the ^{14}C applied, and the time needed to reduce the ^{14}C initially applied to 50% was 5.0 ± 0.7 d (calculated from $\ln 2/k$).

Table 4

Carbon-14-glyphosate mineralized, C-CO₂ expressed as a percentage of the total organic C, and setting parameters for three soils and two cropping sequences using the equation $C_t = C_0 [1 - \exp(-kt)]$, where C_t is the percentage of ¹⁴C-CO₂ or C-CO₂ mineralized at time t , C_0 is the percentage of C potentially mineralizable, k is the daily mineralization rate, and t is time in days.

| Soils | Cropping sequence | Mineralization of glyphosate | | | Mineralization of soil organic C | | |
|----------------|-------------------|---------------------------------|----------------|-----------------|----------------------------------|----------------|-----------------|
| | | ¹⁴ C-CO ₂ | C ₀ | k | C-CO ₂ | C ₀ | k |
| | | % | % | d ⁻¹ | % | % | d ⁻¹ |
| Marcos Juarez | monoculture | 69.1 ± 0.3 | 62.8 ± 1.3 | 0.178 ± 0.018 | 2.8 ± 0.03 | 3.0 ± 0.11 | 0.044 ± 0.003 |
| | rotation | 63.8 ± 0.2 | 57.7 ± 1.2 | 0.170 ± 0.017 | 2.4 ± 0.02 | 2.5 ± 0.09 | 0.053 ± 0.005 |
| Manfredi | monoculture | 68.3 ± 0.3 | 63.1 ± 1.0 | 0.163 ± 0.012 | 3.3 ± 0.03 | 4.1 ± 0.31 | 0.031 ± 0.004 |
| | rotation | 61.6 ± 0.1 | 57.4 ± 1.0 | 0.141 ± 0.011 | 4.3 ± 0.02 | 4.7 ± 0.21 | 0.044 ± 0.004 |
| Pampa de Pocho | monoculture | 65.3 ± 0.5 | 60.9 ± 1.2 | 0.117 ± 0.009 | 3.2 ± 0.03 | 3.0 ± 0.11 | 0.063 ± 0.006 |
| | rotation | 74.3 ± 2.8 | 66.9 ± 1.5 | 0.159 ± 0.017 | 3.2 ± 0.03 | 3.3 ± 0.11 | 0.054 ± 0.005 |

Decreased ¹⁴C-glyphosate mineralization detected in the MJ and M sites relative to the PP site might be associated with increased glyphosate adsorption in the MJ and M soils. We found that the TMA (total microbial activity) was significantly different ($P < 0.01$) among sampling site soils: M > PP > MJ. The M soils, with the highest TMA, did not have the highest ¹⁴C-glyphosate mineralization. Glyphosate mineralization was affected by cropping sequence. At the end of incubation, the ¹⁴C-CO₂ evolved was monoculture MJ = 69% vs. rotation MJ = 63.6% and monoculture Mm = 68% vs. rotation M = 61.7% ($P < 0.05$). These results provide additional support to our interpretations regarding glyphosate mineralization differences detected among study sites, given that monoculture soils showed reduced glyphosate adsorption and a history of glyphosate use.

Carbon-14-Glyphosate Distribution among Mineralized, Extractable, and Nonextractable Residues

The three study sites differed in the distribution of initial radioactivity applied and in the proportion remaining in ER and NER forms. The lower proportion of ER2 and NER in the PP soils corresponded with soil properties involving low sorbent surfaces. Sequential extraction of ER and NER was conducted following 49 d of incubation; consequently equilibrium between soluble and sorbed forms of glyphosate should have occurred. The PP soil contained 19% ER (ER1 + ER2), which clearly contrasted with 30% ER obtained from the M and MJ soils. The ER1 fraction, extracted with water, represented the weakly adsorbed herbicide and on average was <5% of the total ER for the three sample sites. The ER1 from the PP soils was slightly higher than that from the other two sample sites (MJ and M), indicating weak glyphosate adsorption properties and high sorption reversibility. Nonextractable residues constituted a small fraction (4-6%) of the ¹⁴C-glyphosate initially applied. Small differences among soils were observed, such as decreasing order of NER proportions: M > MJ > PP ($P < 0.05$). The M soils showed the highest TMA and NER proportion.

Conclusions

The study of glyphosate retention and degradation processes through a pedoclimatic gradient turned out to be a useful tool to recognize and establish some behavioral patterns. Identification of soil indicators that allow inference of glyphosate behavior is one of the goals in studies of sustainable soil use. We found that along a distance of approximately 280 km, gradual changes in glyphosate behavior were associated with pedoclimatic characteristics. Soil properties associated with soil surface reactivity, such as CEC, WHC, and PWP, increased in from northwest to southeast together with the increase in glyphosate adsorption and the increase in hysteresis of desorption. Changes in the glyphosate distribution between adsorbed and soluble forms establish, in part, a behavior pattern of extractable (ER) and mineralized forms. The extent of glyphosate adsorption and also the hysteresis of desorption were higher in rotation soils than monoculture soils; that is, soils with identical properties exhibited a different glyphosate retention capacity due to the cropping sequence. The results of this study contribute to our understanding of glyphosate behavioral patterns in relation to different edaphoclimatic scenarios and establish criteria for use in reducing potential environmental risks.

3. Assessment and conclusion

Assessment and conclusion by applicant:

The study describes the sorption and degradation behavior of ^{14}C -labelled glyphosate in different agricultural soils from Argentina. Sorption parameters and mineralization of the substance are reported. However, essential parameters are not described, or there are some deviations from current guidelines. In addition, the pedo-climatic conditions do not correspond to EU conditions.

The study is therefore classified as reliable with restrictions (Category 2).

1. Information on the study

| | |
|---|--|
| Data point: | KCP 9.2.4 |
| Report author | Rasmussen, S., et al. |
| Report year | 2015 |
| Report title | Effects of Single Rainfall Events on Leaching of Glyphosate and Bentazone on Two Different Soil Types, using the DAISY Model |
| Document No | Vadose Zone Journal; Advancing Critical Zone Science; Published November 13, 2015 |
| Guidelines followed in study | None |
| Deviations from current test guideline | None |
| GLP/Officially recognised testing facilities | No, not conducted under GLP/Officially recognised testing facilities (literature publication) |
| Acceptability/Reliability: | Reliable with restrictions (Modelling exercise) |

2. Full summary of the study according to OECD format

The purpose of the present modeling study was to contribute to an improved understanding of the mechanisms involved in pesticide leaching during a single rainfall event with temporal variability. Rainfall intensity of the first event after pesticide application has great effect on the amount of pesticide transported to groundwater and subsurface drains, especially in soils containing preferential flow pathways. One way to improve the understanding of single event properties on pesticide leaching is to use a transport model. The soil–plant–atmosphere model Daisy was used to simulate pesticide leaching during and after single rainfall events of different durations and intensities. Designed temporally variable single rainfall events based on the Chicago Design Rain were inserted in the original weather file. A combination of different intensities (13, 20, 24, 28, 34, and 39 mm/h) at different event durations (1, 3, 5, and 9 h) where the intensity peak was placed in the middle of the event were applied, resulting in 24 different design events. The model setup included two different soil types: a coarse sandy soil and a sandy loam containing macropores and subsurface drains. The fates of the herbicides bentazone [3-isopropyl-1*H*-2,1,3-benzothiadiazin-4(3*H*)-one 2,2-dioxide] and glyphosate [*N*-(phosphonomethyl) glycine] were simulated. The leaching dynamics of both pesticides showed high variability at the hourly level, illustrating the importance of high model resolution when estimating pesticide leaching. For the coarse sandy soil different intensities did not appear to have an effect, as pesticide leaching was controlled by event volume. In contrast, results for the sandy loam showed an effect of intensity, especially for glyphosate, at initially wet soil conditions. Short intense events (1 h) resulted in high leaching to drains (1.7% of matrix infiltration) compared to events of longer duration (up to 0.4% of matrix infiltration). This indicates that it might be more prudent to view leaching as a risk that occurs under certain conditions, rather than something that can be averaged.

Materials and Methods

Soils

Two different agricultural soils from Denmark were chosen as model soils—a coarse sandy soil and a sandy loam. The DAISY (deterministic and dynamical two-dimensional soil–plant–atmosphere model developed for simulating agrohydrological systems) parameterization of this location (Jutland, Denmark) originates from Jacobsen (1989), and selected soil properties are illustrated in Table 1. Because the coarse sandy soil is considered completely homogeneous in the Ap and C horizons and contains no biopores or subsurface drains, it is modeled in 1D. The sandy loam is a heterogeneous soil developed in a glacial till in the eastern part of Zealand, Denmark. It shows signs of long-term agricultural use with the development of a plow pan that has a lower hydraulic conductivity than the surrounding soil layers (Petersen et al., 2001).

Table 1. Selected soil characteristics of the two locations, coarse sand and sandy loam, used in the DAISY simulations. Data originate from Jacobsen (1989) and Hansen et al. (2012b).

| Soil type | Horizon | Soil depth | Clay | Silt | Sand | Humus | K_{sat} |
|-------------|---------|------------|------|------|------|-------|--------------------|
| | | cm | % | | | | cm h^{-1} |
| Coarse sand | Ap | 0–30 | 3.8 | 7.2 | 86.7 | 2.3 | 21.7 |
| | C | 30–200 | 2.8 | 2.3 | 94.5 | 0.4 | 92.5 |
| Sandy loam | Ap | 0–25 | 10.4 | 21.6 | 65.1 | 2.9 | 0.174 |
| | Bplow | 25–33 | 14.6 | 21.1 | 62.8 | 1.6 | 0.046 |
| | Br | 33–120 | 21.9 | 19.2 | 57.4 | 1.6 | 0.269 |
| | C | 120–200 | 20.5 | 23.3 | 55.2 | 1.0 | 1.500 |

The sandy loam contains biopores and subsurface tile drains. The drains are placed in a depth of 1.1 m, and 16 m apart, and the biopores are divided into classes according to the depth at which they begin and end in the soil profile. Selected soil properties for this location, which originates from Hansen et al. (2012b) are illustrated in Table 1.

Pesticide Management

Bentazone was applied on 17 June with a rate of 960 g/ha, on grass for cutting. Hence, bentazone is located in the crop canopy and will there be mixed with the first rainfall and washed off the plants when the interception capacity is exceeded. Glyphosate was applied on 30 October at a rate of 1440 g/ha on bare soil (stub after harvesting of maize, *Zea mays* L.) (Table 2). Glyphosate will therefore be located at the soil surface, from where it will enter the soil system together with the first rainfall. The fate of both pesticides was simulated for 4 yr, and their leaching at 2 m depth was logged. For the sandy loam, transport of pesticides into drains was included in the leaching assessment.

Table 2. Pesticide management plan used in the DAISY simulations.

| Rotation year | Crop | Pesticide | Application date | Dosage |
|---------------|------------------------|------------|------------------|-------------------------|
| Warm-up | Spring barley | | | |
| Warm-up | Spring barley | | | |
| Warm-up | Spring barley | | | |
| Warm-up | Spring barley w. grass | | | |
| 1 | Grass | Bentazone | 17 June | 960 g ha ⁻¹ |
| 2 | Grass | | | |
| 3 | Grass | | | |
| 4 | Maize | Glyphosate | 30 October | 1440 g ha ⁻¹ |
| 5 | Spring barley | | | |
| 6 | Spring barley | | | |
| 7 | Spring barley | | | |
| 8 | Spring barley | | | |

Weather Data

The weather file used in the DAISY simulations was provided by University of Copenhagen and originated from Taastrup, Denmark. It contains hourly values of precipitation, temperature, relative humidity, wind speed, and global radiation and covers the period 1999 to 2008 (8 yr). The weather data covered the 8 yr of pesticide tracking in the model simulations (Table 2). To initiate the soil water content in the model, 4 yr of weather data (1999–2003) and a simple spring barley (*Hordeum vulgare* L.) crop rotation were used as a warm-up period before the first pesticide application. The weather record was then reset as the 8 yr of pesticide simulations began (Table 2). The weather of the warm-up period was kept constant, while the weather of the 8 yr of pesticide simulations were permuted.

Artificial Rainfall Events

A single artificial rainfall event was inserted in the weather file 4 d after application of the pesticide. Intermittent rain that occurred between pesticide application and the artificial rainfall event were removed. The artificial event originates from the CDS rain, developed in the 1950s, for the use in city sewage planning. The durations of the events studied were 1, 3, 5, and 9 h combined with six different levels of maximum intensities of 13, 20, 24, 28, 34, and 39 mm/h (Table 3). When the duration increases, the maximum intensity of the event will be displaced to the middle of the event, and small pre- and post-tails of rain will be added to the event compared to a 1-h event (Fig. 1). Hence, the event volume is connected to the event duration, as increased duration results in increased volume.

Table 3. Characteristics of the inserted Chicago Design Storm rain (CDS rain. All combinations of maximum intensities and durations were investigated at eight different initial conditions, and with different post-event weather.

| Max. intensity | Duration | Volume | Repeat interval |
|--------------------|----------|--------|-----------------|
| mm h ⁻¹ | h | mm | yr |
| 13 | 1 | 13 | 1 |
| 13 | 3 | 18 | 1 |
| 13 | 5 | 21 | 1 |
| 13 | 9 | 25 | 1 |
| 20 | 1 | 20 | 5 |
| 20 | 3 | 28 | 5 |
| 20 | 5 | 33 | 5 |
| 20 | 9 | 39 | 5 |
| 24 | 1 | 24 | 10 |
| 24 | 3 | 33 | 10 |
| 24 | 5 | 39 | 10 |
| 24 | 9 | 46 | 10 |
| 28 | 1 | 28 | 20 |
| 28 | 3 | 39 | 20 |
| 28 | 5 | 45 | 20 |
| 28 | 9 | 53 | 20 |
| 34 | 1 | 34 | 50 |
| 34 | 3 | 48 | 50 |
| 34 | 5 | 55 | 50 |
| 34 | 9 | 65 | 50 |
| 39 | 1 | 39 | 100 |
| 39 | 3 | 55 | 100 |
| 39 | 5 | 64 | 100 |

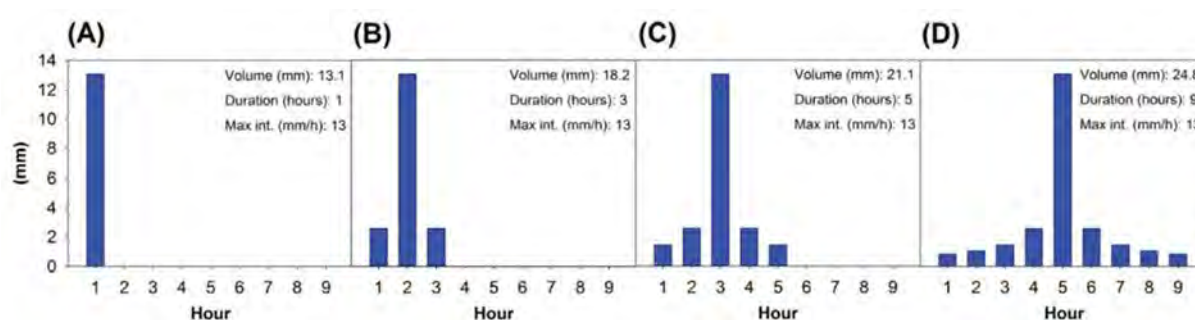


Fig. 1. Examples of Chicago Design Storm rain (CDS-rain) (Kiefer and Chu, 1957), modified by Madsen et al. (2002) and Arnbjerg-Nielsen et al. (2006), inserted in the weather files used in the DAISY simulations. (A) to (D) illustrate the range of event durations investigated and the differences in rain distribution pattern and consequently the differences in total volumes at different durations, with the same maximum intensity.

Results and Discussion

The complete set of total leaching (leaching after 4 yr as percentage of soil input) from the 192 DAISY simulations is illustrated in Fig. 2. A quick overview of the dataset is supplied, as the leaching percentages are shown in a sorted sequence from lowest to highest leaching. It is seen that there is an

effect of soil type on leaching of both pesticides and that bentazone leaching is substantially larger than glyphosate leaching. In the following responsible processes and mechanisms will be described, and where feasible, related to field or laboratory findings. For each of the two soil types, a description of pesticide leaching during the 4-yr simulations (leaching dynamics) will be followed by a clarification of the effects of CDS event structure (event characteristics) and completed with a description of the importance of initial soil water conditions and post-event weather (rotated weather).

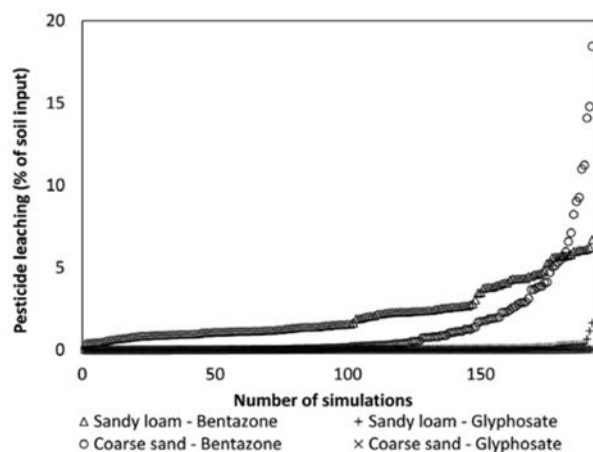


Fig. 2. Overview of all pesticide fate simulations made by the DAISY model. Total bentazone and glyphosate leaching as percentage of soil input (matrix and biopore infiltration), at the coarse sandy and sandy loam soils. The 192 simulations for each pesticide, at each soil type, are sorted from smallest to largest.

Pesticide Leaching in the Coarse Sand—Leaching Dynamics

The pesticides entered the soil with the first rainfall after application and were thereafter transported vertically through the soil profile with the water. Fig. 3 illustrates bentazone and glyphosate leaching (daily values) during 4 yr after pesticide application. The amount of pesticide leaching is calculated at the soil depth of 2 m and is given as the percentage of input to the soil. The average \pm SD of all 24 investigated CDS events are shown together with accumulated net precipitation (precipitation minus evapotranspiration) (Fig. 3). The inserted figure illustrates the negative values of accumulated net precipitation during the first 10 d and the importance of glyphosate leaching the first 5 to 10 d. A seasonality in rainfall is seen, as increased accumulated net-precipitation occurs during autumn and winter.

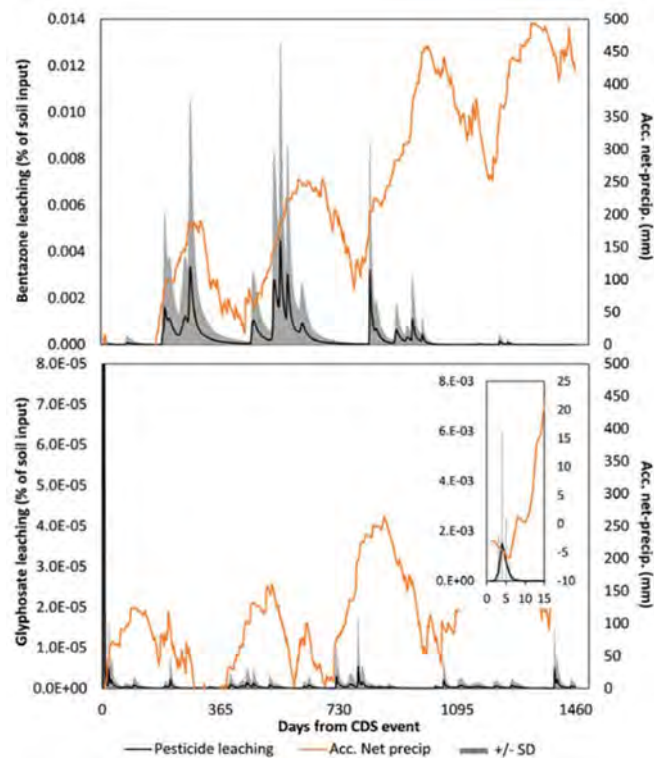


Fig. 3. Four-year pesticide leaching as percentage of soil input (matrix and biopore infiltration) in the coarse sandy soil (daily values). Pesticide leaching is given as an average \pm SD of the 24 different events investigated within Weather Rotation 8. The second y axis shows the accumulated net precipitation (precipitation minus evapotranspiration), with negative values only shown in the inserted figure. The inserted figure also illustrates the full magnitude of glyphosate leaching.

It can be seen that bentazone leaching took place over a 3-yr period, with the highest leaching occurring during winter. Within the first 10 d after the CDS event only $2.7 \times 10^{-5}\%$ of total leached bentazone had reached the 2-m depth, which indicate a limited direct effect of the 24 CDS events. Bentazone was applied 17 June (Table 2), where evapotranspiration most often exceeds the rainfall volume, resulting in dry soil water conditions. The CDS event transports bentazone into the soil profile, but not below the depth of 1 m, where biodegradation is zero in the model. Hence, under these conditions the first rainfall after bentazone application appears of minor importance at the two layered homogeneous coarse sandy soil. In contrast, the direct response of the CDS event on glyphosate leaching (Fig. 3, illustrating variation of the 24 events and effect of WR 8), was found to be substantially larger. Within 10 d after the CDS event 86% of total leached glyphosate had been transported to the 2-m depth. However, total glyphosate leaching ($3.5 \times 10^{-3}\%$ of soil input) is two magnitudes smaller than total bentazone leaching ($4.5 \times 10^{-1}\%$ of soil input), which is a result of the higher sorption properties of glyphosate. Glyphosate was applied 30 October, which is a time of year where the net rainfall is substantially larger than at the time of bentazone application (17 June), resulting in wetter soil water conditions, especially at the top 0.5 m. This means that smaller amounts of rainfall is needed to facilitate the transport of glyphosate, and a direct and visible effect of the CDS events is possible (Fig. 3).

Pesticide Leaching in the Coarse Sand—Effect of Single Event Characteristics

Even though the immediate effect of the CDS events were small (Fig. 3), total bentazone leaching at the coarse sandy soil, showed a systematic response to the 24 investigated CDS events. Bentazone leaching increased with increased duration (1, 3, 5, and 9 h) and maximum intensity (13, 20, 24, 28, 34, and 39 mm/h) of the CDS event. This is illustrated in Fig. 4, where the average \pm SD of total bentazone leaching of all 8 WRs are shown, but divided into event durations and maximum intensities. This was to be expected, as a higher rainfall volume has a higher potential of transporting pesticides. With increased CDS event volume, the pesticide was transported faster through the degradation zone (upper 1 m), which

left less time for degradation. These results also indicate that higher intensities will result in increased leaching percentages. Glyphosate leaching at the coarse sandy soil showed the same pattern as the one found for bentazone, although only small amounts of glyphosate were leached (<0.025% of soil input).

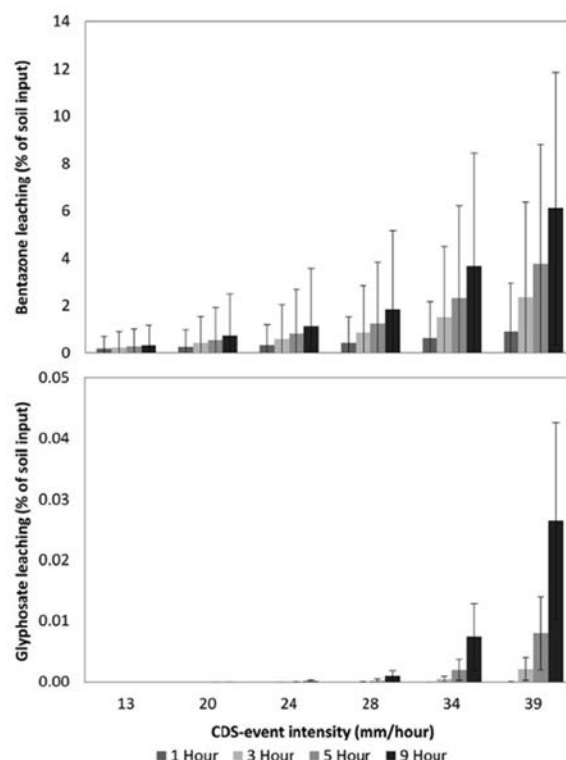


Fig. 4. Average \pm SD of 4 yr accumulated pesticide leaching, based on results from all eight weather rotations, shown as percentage of soil input (matrix and biopore infiltration), in the coarse sandy soil, and as a function of Chicago Design Storm (CDS) event intensity and duration.

Pesticide Leaching in the Coarse Sand—Effect of Rotated Weather

The rotated weather produced different soil water conditions at the time of pesticide application, and different post-CDS event weather, which all may influence the pesticide fate. Fig. 5 illustrates these effects on pesticide leaching, where daily values of leaching are given as a function of CDS event volume, for all 8 WRs. These results indicate that the leaching pattern can be explained by the volume of the CDS event, as the accumulated leaching of especially bentazone produced smooth curves at the coarse sandy soil and showed almost no effect of increased intensity. In the case where intensity had an effect, the curves would be irregular, showing a spread of leaching results. This indicates that the effect of intensity shown in Fig. 4 is solely explained by the increase in volume, as intensity increases. The leached amounts of glyphosate were smaller than those of bentazone and showed a steeper curve. This is due to the high number of low leaching percentages even at relatively high CDS event volumes (up to 50 mm). When event volume exceeds 50 mm, a steep increase in leaching percentages was observed (Fig. 5). The difference between the leaching caused by the different WRs in Fig. 5 is either due to the initial soil water conditions (water conditions at the time of pesticide spraying), the post-event rainfall, or a combination thereof. Bentazone leaching at the coarse sandy soil appeared to be mostly affected by CDS event volume. In the case of glyphosate leaching at the coarse sandy soil, no connection to initial soil water conditions or P_{10} was found, except at WR 3 which had the highest P_{10} and the highest leaching.

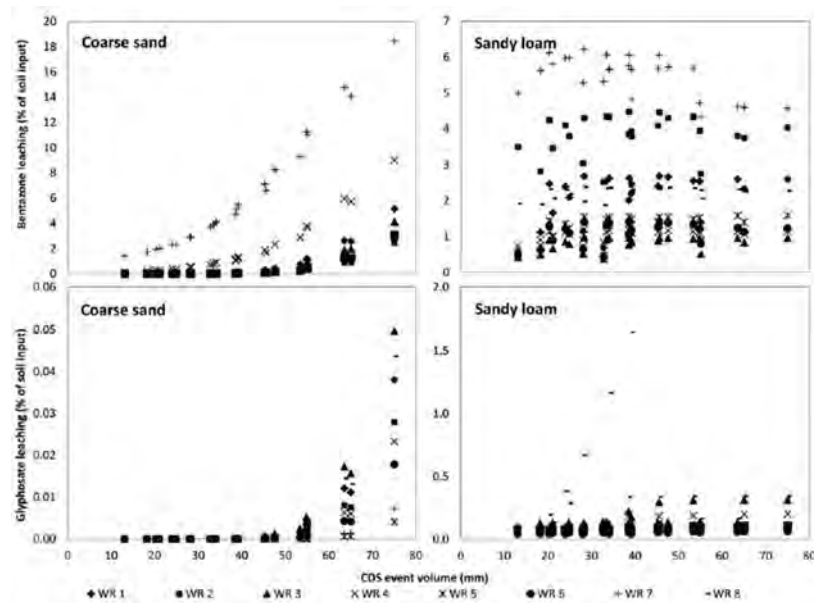


Fig. 5. Four-year cumulative pesticide leaching shown as percentage of soil input (matrix and biopore infiltration), and as a function of Chicago Design Storm (CDS) event volume. Each of the eight weather rotations (WRs) represents a new set of initial soil water conditions and post-CDS event weather conditions. Please note the different scales on the y axis.

Pesticide Leaching in the Sandy Loam—Leaching Dynamics

Fig. 6 constitutes an example of how daily values of pesticide leaching (to drain plus leaching at 2 m depth) evolved over the 4 yr period of which the pesticides were tracked. Average \pm SD of the 24 CDS events from WR 8 is shown. Compared to similar graphs for the coarse sandy soil (Fig. 2), it can be seen that the largest proportion of both pesticides were leached during or shortly after the CDS event, as was the case for glyphosate at the coarse sandy soil. On average, 87% of total bentazone leaching and 75% of total glyphosate leaching occurred within 24 h from the beginning of the CDS event. Hence, the first single rainfall event after pesticide leaching is of considerable importance on the sandy loam, compared to the coarse sandy soil. Even though both pesticides were affected by the CDS event (Fig. 6), it was found that different processes control the leaching of the two pesticides. It was found that a substantial part of drain leached bentazone was transported via biopores leading directly from the surface to the tile drain. A total of 51% of drain leached bentazone (average of the 24 CDS event in WR 8) completely bypassed the soil matrix where sorption would have occurred. The second way of entering biopores via the soil matrix is how glyphosate predominantly migrated. Only 23% of drain leached glyphosate, was transported directly from the soil surface into the biopores, completely bypassing the soil matrix. Further investigation into the transport mechanisms revealed that the agricultural practice was important, in particular the presence of a plant cover in the model setup. Bentazone was applied on grass for cutting, and thus had to be washed off the crop canopy before getting into contact with the soil surface. The CDS event is the first rainfall after pesticide application and is heavy enough to wash bentazone off the canopy and *at the same time* activate the preferential flow pathways where some led directly to the drain. Glyphosate was applied directly to the soil surface and the main fraction entered the soil matrix together with the very first water that hit the surface. When the pesticide had entered the soil matrix it either sorbed to soil particles or followed the water route in dissolved form through the soil matrix into the biopores and from here to the drain pipe. Despite high sorption of glyphosate a small fraction was present as dissolved glyphosate, which was subject to leaching through transport route B. This explains the dependence of amount of water that comes after the maximum intensity in the CDS event: the hour of maximum intensity does not result in relatively higher transport of glyphosate, since the majority of this water is led directly into macropores and thereby bypassing the soil matrix where glyphosate is located.

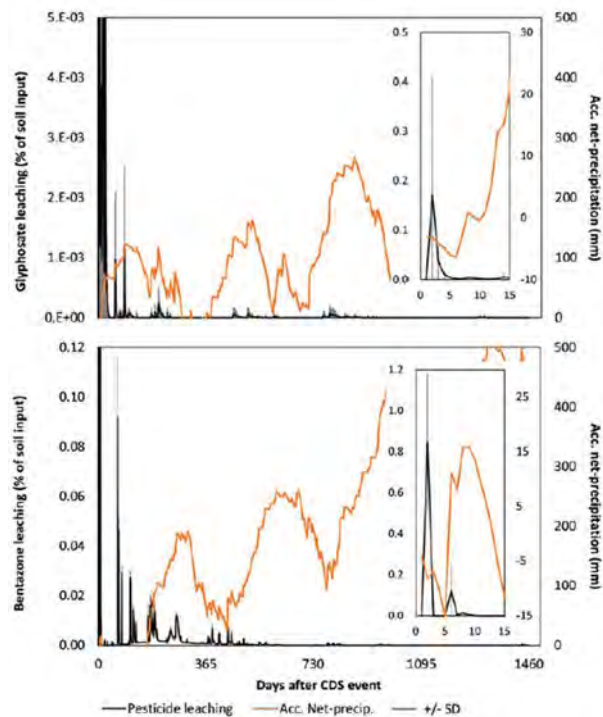


Fig. 6. Four-year pesticide leaching shown as percentage of soil input (matrix and biopore infiltration) in the sandy loam soil (daily values). Pesticide leaching is given as an average \pm SD of the 24 different events investigated within Weather Rotation 8. The second y axis shows the accumulated net precipitation (precipitation minus evapotranspiration), with negative values only shown in the inserted figures.

Pesticide Leaching in the Sandy Loam—Effect of Single Event Characteristics

Bentazone leaching was found to increase as CDS event volume increased. The CDS events of 3, 5, and 9 h caused leaching that tended to level out as CDS event volumes increased. This trend represents the prevailing leaching patterns, but some WRs showed limited effect of CDS event volume. The differences in leaching dynamics between bentazone and glyphosate in the sandy loam (Fig. 7) were also observed at the 4-yr cumulated leaching (Fig. 8). The applied glyphosate was protected against soil infiltration by small rainfall events when located in a litter layer, and a substantial amount of glyphosate was transported via the biopores to the drains during a heavy event that generated preferential flow. Long CDS event durations resulted in high leaching percentages of glyphosate.

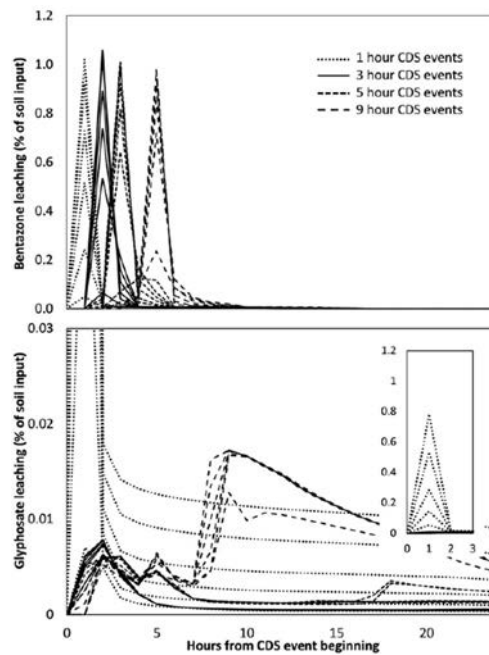


Fig. 7. Four-year pesticide leaching shown as percentage of soil input (matrix and biopore infiltration) in the sandy loam soil (hourly values). Pesticide leaching is shown for each of the 24 different events investigated within Weather Rotation 8, but divided into groups according to the respective Chicago Design Storm (CDS) event duration.

Pesticide Leaching in the Sandy Loam—Effect of Rotated Weather

The smooth curves produced at the coarse sandy soil (Fig. 5) were not reproduced, indicating that CDS event volume alone did not explain the leaching in the sandy loam. The increased bentazone leaching caused by increased CDS event volume (Fig. 8) is not repeated by all WRs, and the effect of CDS event characteristics appear of less importance compared to the effect of initial soil water conditions and post-event weather. Glyphosate leaching appeared to be affected by CDS event intensity to a higher degree than bentazone.

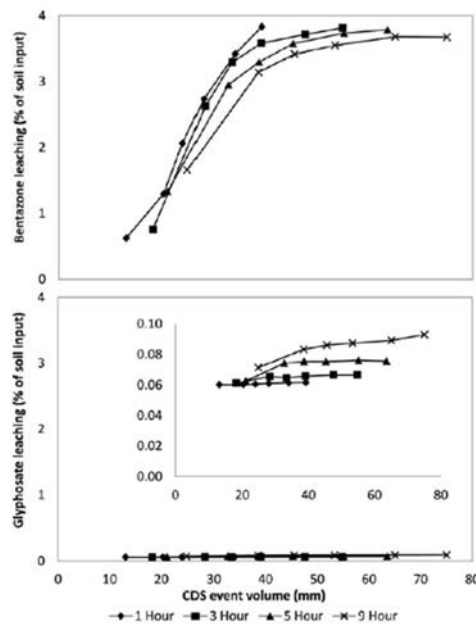


Fig. 8. Four-year accumulated pesticide leaching shown as the percentage of soil input (matrix and biopore infiltration) in the sandy loam and as a function of the Chicago Design Storm (CDS) event volume, Weather Rotation 1.

Simulated Pesticide Concentrations in the Sandy Loam

The simulated concentrations of bentazone and glyphosate in drainage water at WR 8 are shown in Fig. 9. Both pesticide concentrations are seen to peak shortly after the CDS event beginning. Previous studies strongly indicate that glyphosate leaching is highly event driven, where especially rainfall intensity affects the leaching dynamics. High intensity rainfall events occurred as the first rainfall after application at initially wet soil conditions, which supports the findings of this work.

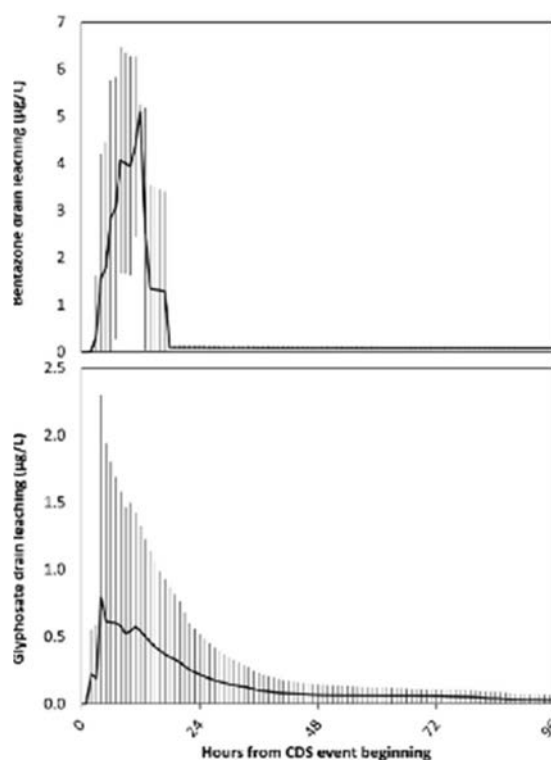


Fig. 9. Pesticide leaching ($\mu\text{g/L}$), during the first 4 d after the Chicago Design Storm (CDS) event in the sandy loam soil. Pesticide leaching is given as an average \pm SD of the 24 different events investigated within Weather Rotation 8. Negative SD values are not shown.

Conclusions

Based on the 192 model simulations, testing the effect on pesticide leaching of duration and intensity of the first rainfall event after pesticide application at an hourly temporal resolution, the following trends were observed: The importance of the first single rainfall event after pesticide application depended highly on soil types. On average, 87% of total bentazone leaching and 75% of total glyphosate leaching occurred within 24 h from the CDS event beginning in the sandy loam. Hence, the first single rainfall event after pesticide leaching is of considerable importance in the sandy loam. Preferential flow transport in the biopores was responsible for this immediate transport of both pesticides. In the coarse sandy soil, the first rainfall event was of minor importance, and the effect was only visible if the soil was relatively wet at the time of application. The influence of rainfall characteristics on pesticide leaching depends on the hydrological conditions of the investigated soil types. In the coarse-textured soil, where non-threshold matrix flow dominates, solute leaching was found to increase with increased rainfall volume, whereas in the sandy loam, varying rainfall intensity also affected pesticide leaching, especially for the strongly sorbing pesticide glyphosate. For strongly sorbing pesticides like glyphosate it might be more prudent to view leaching as a risk that occurs under certain conditions, rather than something that can be averaged. Under most initial conditions glyphosate leaching did not vary much (up to 0.4% of soil input), but at specific initial wet surface conditions glyphosate leaching greatly increased (1.7% of soil input). It may therefore be equally important to have knowledge of the weather preceding the pesticide application, as knowledge of the weather following the pesticide application.

3. Assessment and conclusion

Assessment and conclusion by applicant:

The study describes a modelling experiment for the leaching of glyphosate through two different soil types.

The effect of single rainfall events is analyzed.

The study is classified as reliable with restrictions (Category 2).

1. Information on the study

| | |
|---|---|
| Data point: | KCA 7.1.3.1.1 |
| Report author | Sidoli, P., et al. |
| Report year | 2016 |
| Report title | Glyphosate and AMPA adsorption in soils: laboratory experiments and pedotransfer rules |
| Document No | Environmental Science and Pollution Research (2016) 23:5733–5742 |
| Guidelines followed in study | OECD 106 (2000) |
| Deviations from current test guideline | None |
| GLP/Officially recognised testing facilities | No, not conducted under GLP/Officially recognised testing facilities |
| Acceptability/Reliability: | Reliable with restrictions (Not all parameters reported to check the validity criteria for the study) |

2. Full summary of the study according to OECD format

Adsorption of the herbicide glyphosate and its main metabolite AMPA (aminomethylphosphonic acid) was investigated on 17 different agricultural soils. Batch equilibration adsorption data are shown by Freundlich adsorption isotherms. Glyphosate adsorption is clearly affected by equilibration concentrations, but the nonlinear AMPA adsorption isotherms indicate saturation of the adsorption sites with increasing equilibrium concentrations. $\text{pH}_{\text{CaCl}_2}$ (i.e. experimental pH) is the major parameter governing glyphosate and AMPA adsorption in soils. However, considering $\text{pH}_{\text{CaCl}_2}$ values, available phosphate amount, and amorphous iron and aluminium oxide contents by using a nonlinear multiple regression equation, obtains the most accurate and powerful pedotransfer rule for predicting the adsorption constants for these two molecules. As amorphous iron and aluminium oxide contents in soil are not systematically determined, we also propose a pedotransfer rule with two variables— $\text{pH}_{\text{CaCl}_2}$ values and available phosphate amount—that remains acceptable for both molecules. Moreover, the use of the commonly measured pH_{water} or pH_{KCl} values gives less accurate results compared to $\text{pH}_{\text{CaCl}_2}$ measurements. To our knowledge, this study is the first AMPA adsorption characterization for a significant number of temperate climate soils.

Materials and Methods

Soil properties

Seventeen surface top soils were sampled in different agricultural plots with variable land uses and fertilization practices under intensive agriculture. The sample site is located in a quaternary fluvio-glacial corridor near Lyon in southeastern France. They are loamy to sandy-loamy soils, characterized by a decarbonation state on surface and large amounts of amorphous iron and aluminium oxides issued from the weathering of primary minerals (Table 1). Fresh soil samples were air-dried, sieved to 2 mm, and stored in the dark at 4 °C, before measuring their physicochemical properties. Crystallized oxy-hydroxides (Fe_{DCB} and Al_{DCB}) were extracted by the Mehra-Jackson method (1960), and amorphous oxy-hydroxides (Fe_{ox} and Al_{ox}) by the Tamm method (1992) (Table 1). The experimental 1:5 soil $\text{pH}_{\text{CaCl}_2}$, hereafter referred to as ' $\text{pH}_{\text{CaCl}_2}$ ', was measured in batch supernatants with a pH microelectrode (Inlab Flex-Micro). These soils showed wide ranges of $\text{pH}_{\text{CaCl}_2}$ (5.1 to 7) and clay content (8.9 to 15.3 %) and, except soil 11, contained less than 2 % organic carbon (Table 1).

Chemical reagents and analysis

Glyphosate adsorption was studied with its ^{14}C -radiolabeled form (phosphonomethyl- ^{14}C)-glyphosate (4.36 MBq/mg, radiochemical purity 96.32 %) purchased from Izotop (Hungary). Unlabeled solid glyphosate and AMPA products (purity $\geq 98\%$) were purchased from Dr Ehrenstorfer (CIL Cluzeau, Sainte-Foy la Grande, France). Stock solutions were prepared in MilliQ water (storage at 4 °C for 1 month).

Table 1

Physicochemical properties of studied soils. Crystallized oxy-hydroxides (Fe_{DCB} and Al_{DCB}) and amorphous oxy-hydroxides (Fe_{ox} and Al_{ox}) were extracted by the Mehra-Jackson method (1960) and the Tamm method, respectively

| Soil | pH _{CaCl2} | pH _{water} | pH _{KCl} | Organic C (g kg ⁻¹) | Olsen P (g kg ⁻¹) | Al _{DCB} (g kg ⁻¹) | Fe _{DCB} (g kg ⁻¹) | Al _{ox} (g kg ⁻¹) | Fe _{ox} (g kg ⁻¹) | Clay % | Silt % | Sand % | CEC (meq 100 g ⁻¹) |
|--------------------|---------------------|---------------------|-------------------|------------------------------------|----------------------------------|--|--|---|---|-----------|-----------|-----------|-----------------------------------|
| 1 | 6.8 | 7.7 | 6.8 | 14.1 | 0.10 | 2.1 | 9.9 | 1.7 | 3.1 | 12.3 | 36.4 | 49.1 | 7.6 |
| 2 | 5.1 | 6.1 | 4.9 | 14.0 | 0.05 | 11.1 | 2.7 | 2.2 | 2.7 | 15 | 37.3 | 45.5 | 8.3 |
| 3 | 5.8 | 6.5 | 5.7 | 13.0 | 0.10 | 2.4 | 10.9 | 2.0 | 2.9 | 15.1 | 39.1 | 43.6 | 8.2 |
| 4 | 5.9 | 6.9 | 6.0 | 13.6 | 0.07 | 2.6 | 11.2 | 1.9 | 2.8 | 14.9 | 38.1 | 45 | 8.1 |
| 5 | 5.9 | 7.5 | 6.6 | 16.0 | 0.09 | 2.5 | 12.8 | 2.0 | 2.7 | 15.3 | 41.5 | 40.8 | 8.2 |
| 6 | 5.8 | 7.0 | 6.1 | 14.7 | 0.07 | 2.4 | 11.5 | 1.9 | 2.7 | 15 | 40.3 | 42.5 | 8.3 |
| 7 | 5.9 | 6.9 | 6.1 | 13.4 | 0.08 | 2.2 | 11.5 | 1.8 | 2.6 | 15 | 39 | 44.2 | 8.4 |
| 8 | 6.1 | 7.2 | 6.3 | 8.3 | 0.11 | 1.8 | 8.8 | 1.5 | 2.6 | 11.4 | 34.3 | 52.8 | 6.0 |
| 9 | 6.2 | 7.3 | 6.5 | 14.8 | 0.06 | 2.5 | 13.5 | 2.1 | 3.2 | 15.4 | 36.3 | 45.7 | 8.2 |
| 10 | 5.5 | 6.7 | 5.8 | 17.3 | 0.06 | 2.5 | 11.5 | 2.0 | 2.9 | 14.8 | 35.6 | 47.3 | 7.7 |
| 11 | 7.0 | 8.0 | 7.2 | 23.1 | 0.20 | 1.5 | 8.6 | 1.2 | 3.0 | 11.8 | 42.3 | 42.8 | 9.6 |
| 12 | 6.1 | 7.0 | 6.1 | 16.1 | 0.08 | 2.1 | 11.8 | 1.9 | 3.0 | 13.9 | 34.1 | 49.5 | 8.2 |
| 13 | 5.1 | 6.3 | 5.4 | 12.9 | 0.04 | 10.6 | 2.1 | 1.8 | 2.8 | 14.6 | 40 | 43.8 | 6.6 |
| 14 | 6.2 | 7.3 | 6.5 | 9.2 | 0.08 | 1.6 | 6.8 | 1.3 | 2.2 | 8.9 | 31.5 | 58.1 | 5.0 |
| 15 | 6.3 | 7.4 | 6.5 | 9.1 | 0.12 | 1.6 | 6.9 | 1.4 | 2.1 | 8.9 | 29.5 | 60.4 | 5.6 |
| 16 | 5.4 | 6.5 | 5.6 | 7.2 | 0.11 | 1.8 | 7.7 | 1.5 | 2.5 | 9.7 | 30.6 | 58.3 | 4.4 |
| 17 | 5.9 | 6.7 | 5.9 | 15.0 | 0.14 | 2.0 | 10.4 | 1.7 | 2.7 | 12.7 | 32.4 | 52.7 | 7.6 |
| Mean | 5.9 | 7.0 | 6.1 | 13.6 | 0.09 | 3.1 | 9.3 | 1.8 | 2.7 | 13.2 | 36.4 | 48.4 | 7.4 |
| Standard deviation | 0.5 | 0.5 | 0.5 | 3.7 | 0.04 | 2.8 | 3.2 | 0.3 | 0.3 | 2.2 | 3.7 | 5.9 | 1.4 |
| Min | 5.1 | 6.1 | 4.9 | 7.2 | 0.04 | 1.5 | 2.1 | 1.2 | 2.1 | 8.9 | 29.5 | 40.8 | 4.4 |
| Max | 7.0 | 8.0 | 7.2 | 23.1 | 0.20 | 11.1 | 13.5 | 2.2 | 3.2 | 15.4 | 42.3 | 60.4 | 9.6 |

The glyphosate concentration was obtained by measuring ¹⁴C-glyphosate activity, which was counted with a liquidscintillation analyzer (Packard Tricarb® 2300TR). After adding a scintillator (Aquasafe 300 Plus, Zinsser Analytic), the radioactivity was measured in 2 mL of supernatant. The minimal measured ¹⁴C-glyphosate radioactivity is 30 dpm/mL which corresponds to 0.09 µg/L.

AMPA analysis was done on an Acquity ultra-performance liquid chromatography system (UPLCTM, Waters) interfaced to a triple quadrupole mass spectrometer (Quattro Premier XE, Waters). Due to its low molecular weight, a derivatization step with FMOC-chloride in the presence of a borate buffer is required prior to analysis. Extraction is done online with an SPE cartouche (Oasis HLB 25 µm 2.1×20 mm) before separation in an Acquity UPLC HSS column (T3 1.8 µm×2.1 mm×100 mm). The quantification limit is 0.05 µg/L.

Isotherm adsorption coefficients (K_f)

Sorption experiments were run according to a normalized method (OECD guideline 106, 2000) with a 1/5 soil-weight/solution-volume ratio in 15-mL centrifuge plastic tube. Equilibrium - tested with a 1 mg/L solution - was obtained after 24 h. After 12 h of pre-equilibration with a CaCl₂ solution (0.01 M), the equilibrated soil suspensions were spiked with a pesticide solution and agitated during 24 h (darkness, 20 °C). After centrifugation (3000 rpm, 30 min, 20 °C), the supernatants were filtrated with 0.2 µm cellulose acetate and analyzed for pesticide concentrations. Blanks (each soil without spiking) did not reveal any presence of either molecule in the soils before the experiments. No adsorption was measured on tubes and filters used for batch experiments. The adsorption isotherm was obtained by the relationship between adsorbed concentration per weight (C_s , mg/kg) compared to the equilibrium concentration per volume of solution (C_e , mg/L) according to the Freundlich equation. Six solute concentrations were tested, 0.05, 0.2, 0.5, 1.0, 3.0 and 5.0 mg/L, for both glyphosate and AMPA. For glyphosate, which was studied with its ¹⁴C radiolabeled form, the initial radioactivity was 6000 dpm/mL in tubes. The experiments were run as triplicates. The Freundlich parameters K_f and $1/n_f$ were estimated by using a nonlinear fitting programme (XLStat, Excel 5.0).

Table 2

Experimental Freundlich isotherm coefficients K_{f-exp} ($\text{mg kg}^{-1}(\text{L mg}^{-1})^{-n_f}$) and $1/n_{f-exp}$ (–) for glyphosate and AMPA, and K_f recalculated for averaged $1/n_{f-exp}$ glyphosate ($1/n_{f-avg}=0.93$) and AMPA ($1/n_{f-avg}=0.78$)

| Soils | Glyphosate | | | | | AMPA | | | | |
|--------------------|-------------|---------------|-------|----------------------------|-------|-------------|---------------|-------|----------------------------|-------|
| | K_{f-exp} | $1/n_{f-exp}$ | R^2 | K_f (for $1/n_{f-avg}$) | R^2 | K_{f-exp} | $1/n_{f-exp}$ | R^2 | K_f (for $1/n_{f-avg}$) | R^2 |
| 1 | 34 | 0.86 | 1.00 | 36 | 1.00 | 63 | 0.74 | 1.00 | 67 | 1.00 |
| 2 | 540 | 0.97 | 0.99 | 475 | 1.00 | 392 | 0.80 | 1.00 | 365 | 1.00 |
| 3 | 143 | 0.93 | 1.00 | 143 | 1.00 | 140 | 0.72 | 1.00 | 162 | 1.00 |
| 4 | 92 | 1.09 | 1.00 | 73 | 0.99 | 212 | 0.79 | 1.00 | 206 | 1.00 |
| 5 | 135 | 0.92 | 0.99 | 139 | 1.00 | 226 | 0.81 | 1.00 | 208 | 1.00 |
| 6 | 132 | 0.90 | 0.99 | 140 | 0.99 | 191 | 0.80 | 1.00 | 183 | 1.00 |
| 7 | 101 | 0.90 | 1.00 | 106 | 0.99 | 143 | 0.75 | 1.00 | 154 | 1.00 |
| 8 | 99 | 0.94 | 1.00 | 97 | 1.00 | 119 | 0.81 | 1.00 | 111 | 1.00 |
| 9 | 107 | 0.91 | 1.00 | 110 | 1.00 | 158 | 0.81 | 0.99 | 147 | 0.99 |
| 10 | 233 | 0.94 | 1.00 | 230 | 1.00 | 242 | 0.77 | 1.00 | 253 | 1.00 |
| 11 | 32 | 0.83 | 1.00 | 34 | 1.00 | 33 | 0.78 | 1.00 | 33 | 1.00 |
| 12 | 91 | 0.94 | 1.00 | 89 | 1.00 | 134 | 0.82 | 1.00 | 122 | 1.00 |
| 13 | 285 | 0.99 | 0.99 | 243 | 0.99 | 284 | 0.79 | 1.00 | 210 | 1.00 |
| 14 | 42 | 0.98 | 1.00 | 40 | 1.00 | 91 | 0.80 | 1.00 | 87 | 1.00 |
| 15 | 41 | 0.88 | 1.00 | 43 | 1.00 | 56 | 0.73 | 1.00 | 61 | 1.00 |
| 16 | 233 | 0.94 | 1.00 | 229 | 1.00 | 198 | 0.78 | 1.00 | 198 | 1.00 |
| 17 | 111 | 0.97 | 1.00 | 103 | 1.00 | 107 | 0.82 | 1.00 | 99 | 1.00 |
| Min | 32 | 0.83 | | 34 | | 33 | 0.72 | | 33 | |
| Max | 540 | 1.09 | | 475 | | 392 | 0.82 | | 365 | |
| Mean | 144 | 0.93 | | 137 | | 164 | 0.78 | | 157 | |
| Standard deviation | 121 | 0.06 | | 106 | | 88 | 0.03 | | 79 | |

Parametric linear and nonlinear regression for pedotransfer rule determination

The relationship between the K_f parameter and soil properties was studied for each pesticide (XLStat, Excel 5.0) by multiple linear and nonlinear regression analyses.

Results and discussion

Freundlich adsorption isotherms

The Freundlich isotherm equation adjusts accurately the experimental data ($R^2 > 0.99$). High experimental glyphosate K_f values, K_{f-exp} , were obtained, ranging between 32 and 540 $\text{mg/kg}(\text{L/mg})^{-n_f}$ (Table 2) in agreement with previous studies. In the case of AMPA, K_{f-exp} values between 33 and 392 $\text{mg/kg}(\text{L/mg})^{-n_f}$ (Table 2) are in the same high adsorption range as glyphosate.

Table 3

| Glyphosate and AMPA K_f coefficients calculated by multiple nonlinear regression from Eq. (2): $K_f = C \cdot e^{\sum_{i=1}^n a_i X_i}$ | | | | | | | | | |
|---|------------------------------|------------------------------|-------------------|---------------------|-------------------------------|--|--|-------------|------|
| Soil variables X_n | Constant | pH measurements | | | Olsen P (g kg ⁻¹) | Al _{ox} (g kg ⁻¹) | Fe _{ox} (g kg ⁻¹) | R^2 | |
| | | 1:5 soil pH _{CaCl2} | pH _{KCl} | pH _{water} | | | | | |
| Regression coefficient values | C | a ₁ | a' ₁ | a'' ₁ | a ₂ | a ₃ | a ₄ | | |
| 4 variables (pH, Olsen P, Al_{ox}, Fe_{ox}) | | | | | | | | | |
| Glyphosate | 5.1 × 10⁻⁵ | -1.7 | | | -1.1 | -0.4 | 1.0 | 0.94 | |
| | 3.6 × 10 ⁻⁵ | | | -1.25 | | -5.6 | -0.1 | 0.1 | 0.65 |
| | 1.3 × 10 ⁻⁶ | | | | -1.30 | -7.3 | -0.4 | 0.3 | 0.61 |
| AMPA | 1.8 × 10⁻⁴ | -0.9 | | | -4.4 | 0.6 | -0.1 | 0.92 | |
| | 3.6 × 10 ⁻³ | | | -0.50 | | -5.4 | 1.3 | -0.7 | 0.81 |
| | 3.8 × 10 ⁻³ | | | | -0.40 | -5.4 | 1.3 | -0.8 | 0.78 |
| 2 variables (pH, Olsen P) | | | | | | | | | |
| Glyphosate | 1.9 × 10 ⁻⁶ | -1.6 | | | -2.6 | | | 0.88 | |
| | 3.5 × 10 ⁻⁵ | | | -1.24 | | -5.3 | | | 0.65 |
| | 6.7 × 10 ⁻⁵ | | | | -1.17 | -6.0 | | | 0.60 |
| AMPA | 6.1 × 10 ⁻⁴ | -0.9 | | | -7.7 | | | 0.88 | |
| | 2.1 × 10 ⁻⁴ | | | -0.7 | | -9.6 | | | 0.73 |
| | 3.2 × 10 ⁻⁴ | | | | -0.7 | -9.8 | | | 0.70 |
| 1 variable (pH) | | | | | | | | | |
| Glyphosate | 1.33 × 10 ⁻⁶ | -1.59 | | | | | | 0.82 | |
| | 2.23 × 10 ⁻⁵ | | | -1.24 | | | | | 0.61 |
| | 2.74 × 10 ⁻⁵ | | | | -1.12 | | | | 0.51 |
| AMPA | 4.67 × 10 ⁻⁴ | -0.97 | | | | | | 0.69 | |
| | 1.18 × 10 ⁻⁴ | | | -0.63 | | | | | 0.37 |
| | 1.18 × 10 ⁻⁴ | | | | -0.63 | | | | 0.37 |

For both molecules, the pedotransfer rule including four variables and the simplified rule including two or one variable(s) are calculated for pH_{CaCl2}, pH_{KCl} or pH_{water}. Value parameters corresponding to the pedotransfer rule including the four pH_{CaCl2}, Olsen P, Al_{ox} and Fe_{ox} variables are indicated in bold

These values are consistent with those obtained by Baez et al. (2015) for molisols and alfisols. Experimental values of the $1/n_{f-exp}$ coefficients vary between 0.83 and 1.09 for glyphosate, and between 0.72 and 0.82 for AMPA. As the $1/n_{f-exp}$ values are different, the glyphosate and AMPA K_{f-exp} datasets cannot be compared directly. Indeed, even if the K_{f-exp} value is similar, the isotherm can be very different because of the $1/n_{f-exp}$ value. For each molecule, the $1/n_{f-exp}$ values had a low standard deviation, allowing to calculate an average $1/n_{f-exp}$ value, i.e. $1/n_{f-avg}$, of 0.93 (± 0.06) and 0.78 (± 0.03) for glyphosate and AMPA, respectively (Table 2). New K_f Freundlich coefficients were recalculated for each soil by using this averaged $1/n_{f-avg}$ value (Table 2). For both molecules, this second fit to the Freundlich equation is very precise ($R^2 \geq 0.99$) and allows the comparison between soils. For AMPA, the $1/n_{f-avg}$ value of less than one (i.e. 0.78) indicates that adsorption is strongly limited by the availability of sorption sites. However, the high glyphosate $1/n_{f-avg}$ value of 0.93 means that adsorption is less governed by the availability of adsorption sites than AMPA. Therefore, despite the similar atomic composition of glyphosate and AMPA, they probably do not sorb in the same way onto the studied soils.

Pedotransfer rule for glyphosate and AMPA adsorption prediction

Regression analysis was restricted to soils with a higher experimental pH_{CaCl2} than both glyphosate pK_{a3} and AMPA pK_{a2}, i.e. pH_{CaCl2} > 5.4. This limitation allowed defining adsorption rule when the same ionic form of either glyphosate or AMPA dominates in solution. Thus, soils 2 and 13 (pH_{CaCl2} values = 5.1) were excluded from the data analysis. First, a linear multiple regression was tested to relate K_f to every combination of measured soil properties, but the adjustment accuracy was very weak ($R^2 < 0.75$). In our study, nonlinear consideration sharply improves the fit of both glyphosate and AMPA K_f ($R^2 > 0.92$). Of the ten variables studied, nonlinear regression analysis appears optimized when considering the four variables: pH_{CaCl2} value, available phosphate, and amorphous aluminium and iron oxide amount (Table 3 and Fig. 1), for both glyphosate and AMPA K_f adsorption coefficients. As in earlier studies, the highest correlation was found between glyphosate K_f and pH - in our study pH_{CaCl2} - (Table 4). For the pH_{CaCl2} here studied (between 5.4 and 7.0), deprotonation of the phosphonic group results in the dominant glyphosate net-2⁻ (2⁻) and dominant AMPA net-1⁻ charged (1⁻) forms (Fig. 2). For soils with high pH

values, high repulsion forces with negative charges act on the amorphous oxide surfaces and sorption is reduced. In the regression analysis, both glyphosate and AMPA K_f values positively correlate with amorphous iron and aluminium oxides (Table 4), with higher correlations calculated for amorphous aluminium oxides that probably are more reactive in the studied soils. A negative correlation between available phosphate and glyphosate K_f values is observed (Table 4) where both molecules compete for the same adsorption sites on oxide surfaces, thus reducing glyphosate adsorption in the presence of phosphate (Gimsing et al. 2004b).

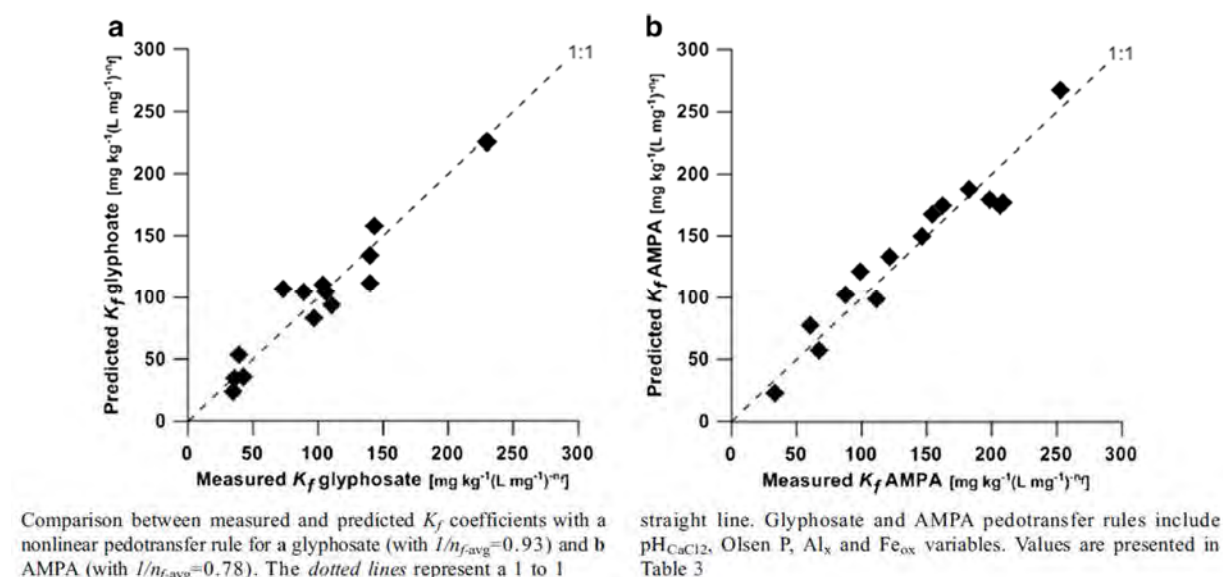
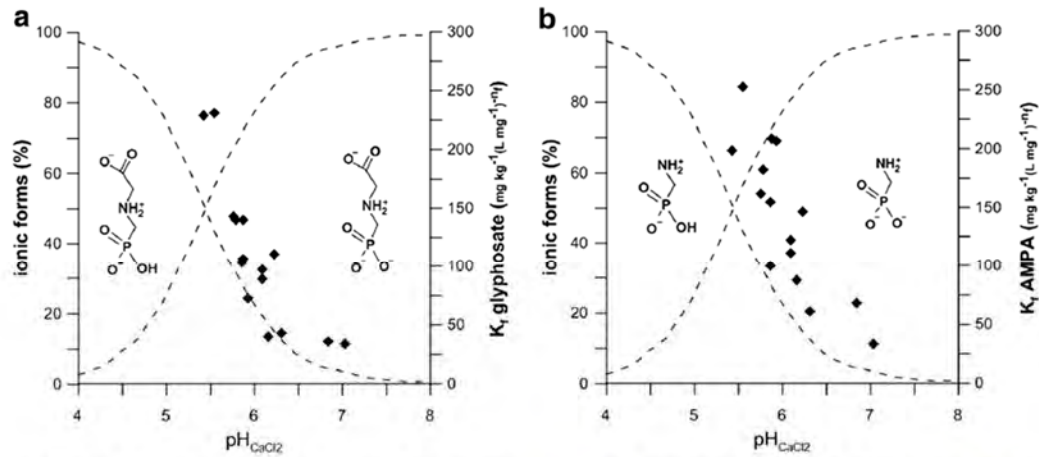


Figure 1

A negative correlation between AMPA K_f values and available phosphate suggests a similar competition for adsorption on oxide surface sites by reducing AMPA sorption when phosphate is present. The more strongly negative correlation between phosphate and K_f values for AMPA than for glyphosate (Table 4) indicates a higher competitive adsorption between phosphate and AMPA than glyphosate.

To evaluate the sensitivity of the variables affecting the pedotransfer rule, the number of variables was initially reduced to two dominant parameters, i.e. $\text{pH}_{\text{CaCl}_2}$ and available phosphate amount. The resulting equation explains 88 % of the variations in the K_f of glyphosate and AMPA (see R^2 , Table 3). Considering only variable $\text{pH}_{\text{CaCl}_2}$ - the most significant of all four variables – decreases the accuracy adjustment for AMPA (R^2 0.69, Table 3), whereas that for glyphosate is only slightly modified (R^2 0.87, Table 3). Thus, it seems possible to arrive at an acceptable estimate of glyphosate adsorption with an equation with just one variable, i.e. $\text{pH}_{\text{CaCl}_2}$, whereas for AMPA, the two variables $\text{pH}_{\text{CaCl}_2}$ and available phosphate amount are needed.



Distribution of Freundlich coefficients K_f as a function of $\text{pH}_{\text{CaCl}_2}$ and dominance of dissociated glyphosate forms (a) and dissociated AMPA forms (b) in solution. Bjerrum diagram taken from (Sheals et al.

2002) for glyphosate (a) and same diagram suggested as hypothesis for AMPA (b). Glyphosate $\text{pK}_{\text{a}_3}=5.46$ (Tomlin 1997), AMPA $\text{pK}_{\text{a}_3}=5.4$ (Chen et al. 2009)

Figure 2

Constraints in applying pedotransfer adsorption equations

To verify the accuracy of the proposed sorption multiple regression, as Paradelo et al. 2015 showed that this might be dependent upon the study site, we collected published data concerning pedotransfer rules for testing them in our model. To our knowledge, AMPA adsorption instead of glyphosate sorption is rarely described in the literature. Nevertheless, none of the published work describes all four variables - $\text{pH}_{\text{CaCl}_2}$, available phosphate, and amorphous iron and aluminium contents - for several soils. We thus carried out an in-depth study on the effect of the pH-measuring method on predicting the glyphosate K_f (Table 3). The parameters for the adsorption equations with four and two variables, or even one variable, were recalculated for pH_{water} or pH_{KCl} values, as these are more commonly measured parameters than experimental $\text{pH}_{\text{CaCl}_2}$. We then did the same work for AMPA equations as a comparison. The choice of pH clearly affected the accuracy of an equation with four variables, as R^2 varied from 0.94 with $\text{pH}_{\text{CaCl}_2}$ to ≤ 0.65 with pH_{water} and pH_{KCl} for glyphosate, and from 0.92 to ≤ 0.81 for AMPA. This decrease in the adjustment accuracy was obviously also noted for regressions with two variables - R^2 going from 0.88 to ≤ 0.65 for glyphosate and from 0.88 to ≤ 0.73 for AMPA—and one variable (R^2 going from 0.88 to ≤ 0.61 for glyphosate and from 0.69 to ≤ 0.37 for AMPA). Glyphosate K_f coefficients are much more affected by the pH measurement method than those of AMPA, but the pH variable in exponential glyphosate equations is systematically associated with higher correlation coefficients than in the AMPA ones (Table 3). These results clearly show that the type of pH measurement plays a crucial role for the prediction of glyphosate and AMPA adsorption coefficients. Since no simple relationship can be established between experimental $\text{pH}_{\text{CaCl}_2}$ and pH_{water} (R^2 0.76) or pH_{KCl} (R^2 0.80), a model validation for glyphosate cannot be based on available published data.

Table 4

Correlation matrix of K_f glyphosate ($1/n_{f\text{-avg}}=0.93$) and K_f AMPA ($1/n_{f\text{-avg}}=0.78$) with soil parameters by multiple nonlinear regression

| Variables | $\text{pH}_{\text{CaCl}_2}$ | Olsen P (%) | Al_{ox} (%) | Fe_{ox} (%) |
|------------------|-----------------------------|-------------|-----------------------------|-----------------------------|
| K_f glyphosate | -0.83 | -0.36 | 0.43 | 0.05 |
| K_f AMPA | -0.82 | -0.67 | 0.68 | 0.10 |

Conclusions

High adsorption coefficients calculated for glyphosate and AMPA molecules depend upon the experimental $\text{pH}_{\text{CaCl}_2}$ value (1:5 soil/solution), the available phosphate content, and the amorphous aluminium- and iron oxide contents. These four key soil parameters combined in an exponential regression equation provide a precise description of a pedotransfer rule for K_f prediction. To our knowledge, our AMPA dataset contains the first published data for adsorption on a significant number of natural soils. Because of low $1/n_f$ values, prediction of the AMPA K_f is strongly related to the soil-solution concentration, contrary to glyphosate. Changes in pH strongly affect adsorption by modifying the ionic state of glyphosate and AMPA and the available amorphous oxide surface sorption sites. Phosphate competes with both molecules for adsorption, but more strongly with AMPA. Considering only the two variables, $\text{pH}_{\text{CaCl}_2}$ and available phosphate content, leads to a satisfactory prediction of the adsorption constants. For both molecules, $\text{pH}_{\text{CaCl}_2}$ is the most reliable explanatory variable. However, $\text{pH}_{\text{CaCl}_2}$ is only rarely measured during batch experiments, even though most of such experiments use CaCl_2 as the solute. Replacing $\text{pH}_{\text{CaCl}_2}$ by pH_{KCl} or by pH_{water} - that are more frequently measured in soils - as the variable in the pedotransfer rule does not allow adjusting K_f with sufficient precision. Since simple relation does not exist between pH_{KCl} and $\text{pH}_{\text{CaCl}_2}$ - or between pH_{water} and $\text{pH}_{\text{CaCl}_2}$ - a complementary soil characterization with $\text{pH}_{\text{CaCl}_2}$ value therefore appears necessary for the application of the pedotransfer rule. However, such a measurement is easier and faster than the implementation of sorption experiments. The acquisition of supplementary data on various soils will lead to a better validation of the pedotransfer rules for glyphosate and AMPA. Finally, the strong adsorption observed in the studied soils, which are rather depleted in organic carbon, takes place on mineral fractions. Hence, the—little studied—geological materials present in the unsaturated zone might also strongly adsorb glyphosate and AMPA. The adsorption of these molecules on such materials should thus be studied as well.

3. Assessment and conclusion

Assessment and conclusion by applicant:

The study describes and sorption experiment with glyphosate on 17 soils from France. The OECD 106 guideline was considered. However, not all parameters were reported to check the validity of the study. The study is therefore classified as reliable with restrictions (Category 2).

1. Information on the study

| | |
|---|--|
| Data point: | KCA 7.1.3.1.1, KCA 7.1.3.1.2 |
| Report author | Skeff, W., et al. |
| Report year | 2018 |
| Report title | Adsorption behaviors of glyphosate, glufosinate, aminomethylphosphonic acid, and 2-aminoethylphosphonic acid on three typical Baltic Sea sediments |
| Document No | Marine Chemistry 198 (2018) 1–9 |
| Guidelines followed in study | None |
| Deviations from current test guideline | No |
| GLP/Officially recognised testing facilities | No, not conducted under GLP/Officially recognised testing facilities |
| Acceptability/Reliability: | Reliable with restrictions (no agricultural conditions, not sufficient data to check validity of the results) |

2. Full summary of the study according to OECD format

A batch experiment was conducted to study the adsorption behaviors of glyphosate, glufosinate, aminomethylphosphonic acid (AMPA), and 2-aminoethylphosphonic acid (2-AEP) in marine sediments (mud, silt, and sand) from the Baltic Sea. The experiment took into account the influence of pH, salinity, and temperature on the adsorption behaviors of the studied compounds. In contrast to glufosinate, glyphosate exhibited an adsorption affinity for the three types of sediments. AMPA and 2-AEP showed similar adsorption behaviors on mud and silt, while their adsorption on sand was negligible. The equilibrium adsorption data for glyphosate, AMPA, and 2-AEP on mud and silt fit well with the linear partitioning and Freundlich isotherms, whereas the data for glyphosate on sand could only be fitted with the Freundlich isotherm. The Freundlich distribution coefficients (k_f) were in the range of 6.1–259.5 L/kg for glyphosate, 9.2–39.5 L/kg for AMPA, and 7.7–38.5 L/kg for 2-AEP under the experimental conditions of pH 8.1, temperature = 21 °C, and a salt concentration of 8 g/L. The adsorption kinetic was better described by the pseudo-second-order than the pseudo-first-order model, suggesting chemisorption as the adsorption mechanism. The order of adsorption of the compounds on the sediments was: glyphosate > AMPA ≥ 2-AEP > glufosinate. The adsorption capacity of sediments followed the sequence: mud > silt > sand. Increasing the pH, salinity, or temperature of the solution significantly reduced the adsorption capacity of the compounds. The data obtained in this study provide valuable information on the fate and distribution of the investigated phosphonates in the Baltic Sea.

Materials and methods

Chemicals and reagents

Standards of glyphosate, a glyphosate internal standard (1-2-¹³C₂¹⁵N glyphosate), AMPA, an AMPA internal standard (¹³C ¹⁵N AMPA), and glufosinate were purchased from Dr. Ehrenstorfer GmbH (Augsburg, Germany). 2-AEP was supplied by Sigma-Aldrich (Taufkirchen, Germany). Stock solutions of these compounds, except the internal standards, were prepared in polypropylene volumetric flasks at a concentration of 100 mg/L by dissolving 5 mg of each compound in 50 mL of LC-MS grade water (VWR International GmbH, Darmstadt, Germany). The stock solutions were stored at 5 °C in the dark. A stock solution (66.6 mM) of 9-fluorenylmethyl chloroformate (FMOC-Cl) (purity 99.0 %, Sigma-Aldrich) was prepared by dissolving 1 g in 58 mL of acetonitrile (Walter-CMP GmbH, Kiel, Germany). Borate buffer at pH 9 was prepared by dissolving 1 g of sodium tetraborate decahydrate (Sigma-Aldrich) in 50 mL of Milli-Q water (Merck KGaA, Darmstadt, Germany). Artificial sea salt, contains all 70 trace elements found in natural seawater in the exact proportions found in nature, was purchased from Tropic Marin®, Germany. Chloroform was supplied by VWR AnalaR Normapur (Germany).

Sediment collection and characterization

Three types of sediment typical of the Baltic Sea were collected from the German Baltic Sea (Figure 1) which are: S1 from Arkona basin (54° 50' N, 13° 30' E), S2 from Tromper Wiek (54° 39' N, 13° 35' E), and S3 from Oder Bank (54° 04' N, 14° 03' E). The sediments were collected using a multiple corer during research cruise EMB76, in June 2014. Samples of the uppermost sediment were sealed in glass jars, stored at -20°C until dry. No sieving was done but large items such as stones, leaves, grass and animals were removed and the samples were manually homogenized. The bulk sediments were freeze-dried using a Chaist ALPHA 1-4 LD freezer dryer and used as sorbents in this study. The grain sizes of the sediments were determined using a CILAS 1180 particle size analyzer. The TOC content of the sediments was analyzed with an elemental analyzer according to (Leipe et al., 2011). The major and trace elements in the sediments were measured using inductively coupled plasma optical emission spectrometry after acid total digested of the samples. The sediment grain sizes were distributed among the different classes: clay (<2 µm), silt (2-63 µm), and sand (>63 µm). The sediment S1 contained 6.6 % clay, 92.3 % silt, and 1.1 % sand, with a median grain size 20.1 µm. The sediment S2 contained 3.6 % clay, 69.9 % silt, and 26.5 % sand, with a median grain size 41.2 µm. The sediment S3 contained 1.7 % clay, 10.7 % silt, and 87.6 % sand, with a median grain size 156.8 µm. The sediment S1, with organic-rich silt-size sediments, was classified as mud, while the sediment S2 as silt and the sediment S3 as fine sand. The sediment TOC, total phosphorus, and major and trace elements followed the order: mud > silt > fine sand.

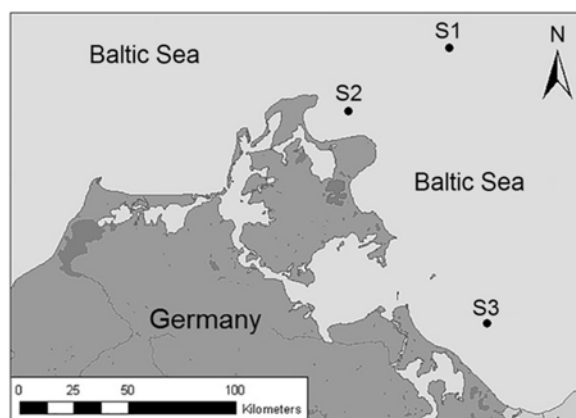


Figure 1. Location of the sampling stations in the German Baltic Sea. The station S1 is in Arkona basin, S2 in Tromper Wiek, and S3 in Oder Bank.

Batch sorption experiment

To investigate the possible adsorption of the analytes onto the walls of the centrifuge tubes, the hydrolysis and degradation of the test compounds during the experiment, a control set of tubes was established in which sediment-free artificial seawater samples were spiked with 250 µg of the analytes/L for 48 h. An additional set of tubes containing sediments with unspiked artificial seawater controlled for possible desorption and the contamination of the sediments and media with the target compounds.

To initiate the experiment, artificial seawater was prepared at a salt concentration of 8 g/L. The pH of the solution was 8.1, measured using a conductivity meter (WTW Inolab cond[®] 720, Germany). Chloroform (0.1 %) was added to the media to inhibit microbial activity. 1 g dry weight of each sediment type was distributed in 15-mL polypropylene centrifuge tubes and mixed with 10 mL of artificial seawater. The tubes were mechanically shaken and incubated for at least 2 days, after which the samples were centrifuged (Megafuge 1.0, Heraeus Instruments) for 3 min at 2500 rpm. Then, 8 mL of each supernatant was transferred to a sediment-free polypropylene centrifuge tube. The samples were then spiked with the target compounds, well shaken at 300 rpm using a mechanical shaker, and 200 µL were then drawn and analyzed for their initial concentrations of the compounds. Thereafter, the spiked medium was returned to the respective sediment tube, which was then vigorously shaken. This process was conducted in order (i) to avoid any possible adsorption of the compounds onto the sediments at the start of the experiment (T = 0 h) and (ii) to allow the analysis of the phosphonates in same sample matrices during the experimental time, whereas a variety of sample matrices might lead to analytical

errors. The experiment was conducted for 48 h at room temperature (21°C), with samples from the aqueous phase taken for analysis at 0, 1, 3, 5, 7, 24, and 48 h. The phosphonates were tested at the following concentrations: 120, 300, 600, 900, and 1200 µg/L. All experiments were performed in duplicate and each sample was measured in triplicate. The target compounds were measured in the aqueous phase. The amounts adsorbed onto the sediments (q_t , µg/g) at time t were calculated according to Eq. (1):

$$q_t = (c_0 - c_t)v/m \quad (1)$$

where c_0 is the initial concentration (µg/L), c_t is the concentration at time t (µg/L), v is the volume of the solution (L), and m is the dry mass of the sediment (g).

Analysis of organophosphonates

A volume of 200 µL of each supernatant was transferred to 2-mL reaction tubes (Eppendorf, Germany) and diluted to 700 µL using LC-MS grade water. The samples were then treated with 100 µL of the glyphosate and AMPA internal standard solutions, prepared in the same matrix, to obtain a final concentration of 15 µg/L. To derivatize the samples, the pH was adjusted to 9 using 100 µL of 0.07 M borate buffer, after which 100 µL of 33.3 mM FMOC-Cl in acetonitrile was added. The samples were shake-incubated at room temperature for 4 h to allow complete derivatization, filtered through a 45-µm Phenex-RC 15-mm syringe filter (Phenomenex, Germany), and analyzed by LC-MS/MS according to a previously described method (Skeff et al., 2015, 2016). Glyphosate was quantified using the glyphosate internal standard, and AMPA, glufosinate, and 2-AEP using the AMPA internal standard.

Statistical analysis

All adsorption experiments were conducted in duplicate, and the measurements in triplicate. The adsorption study measured the initial and equilibrium concentrations of the target compounds. A p -value <0.05 was considered to indicate statistical significance. A one-way ANOVA followed by a Holm-Sidak post-hoc test was carried out using SigmaPlot software (version 13.0, Systat Software Inc.).

Results

Control experiments

A successful adsorption investigation requires the proper controls to rule out both contamination of the aqueous phase or adsorbents with the sorbates and the loss of the sorbates due either to their degradation during the experiment or their adsorption onto the tubes. Controls for both possibilities were therefore established. Data from the first control experiment, in which the compounds were incubated in artificial seawater without sediments, showed a high degree of measurement stability and thus high biological stability of the sorbates during the 48 h and negligible adsorption onto the tubes as well. Furthermore, the stable measurements indicate that the C-P bonds in the organophosphonates are relatively stable and no hydrolysis occurs. Data from the second control experiment, in which the sediments were incubated without sorbates, failed to show the compounds in the aqueous phase and thus confirmed the lack of contamination or desorption. The results of both control experiments demonstrated the validity of the adsorption study.

Kinetic studies and models

The mechanism of glyphosate, glufosinate, AMPA, and 2-AEP absorption onto marine sediments was examined in kinetic studies. The q_t (µg/g) values of glyphosate, AMPA, and 2-AEP between 0 and 48 h are shown in Figure 2. Whereas glyphosate had an affinity for all three types of sediments, AMPA and 2-AEP adsorbed to mud and silt but not sand. Glufosinate concentrations measured in the aqueous phase remained comparable during the 48 h of the experiment, indicating the lack of significant adsorption ($p > 0.05$) onto the sediments. The presence of a methyl group on the phosphonate of glufosinate might obstruct the formation of surface complexes, thus limiting its adsorption compared to glyphosate.

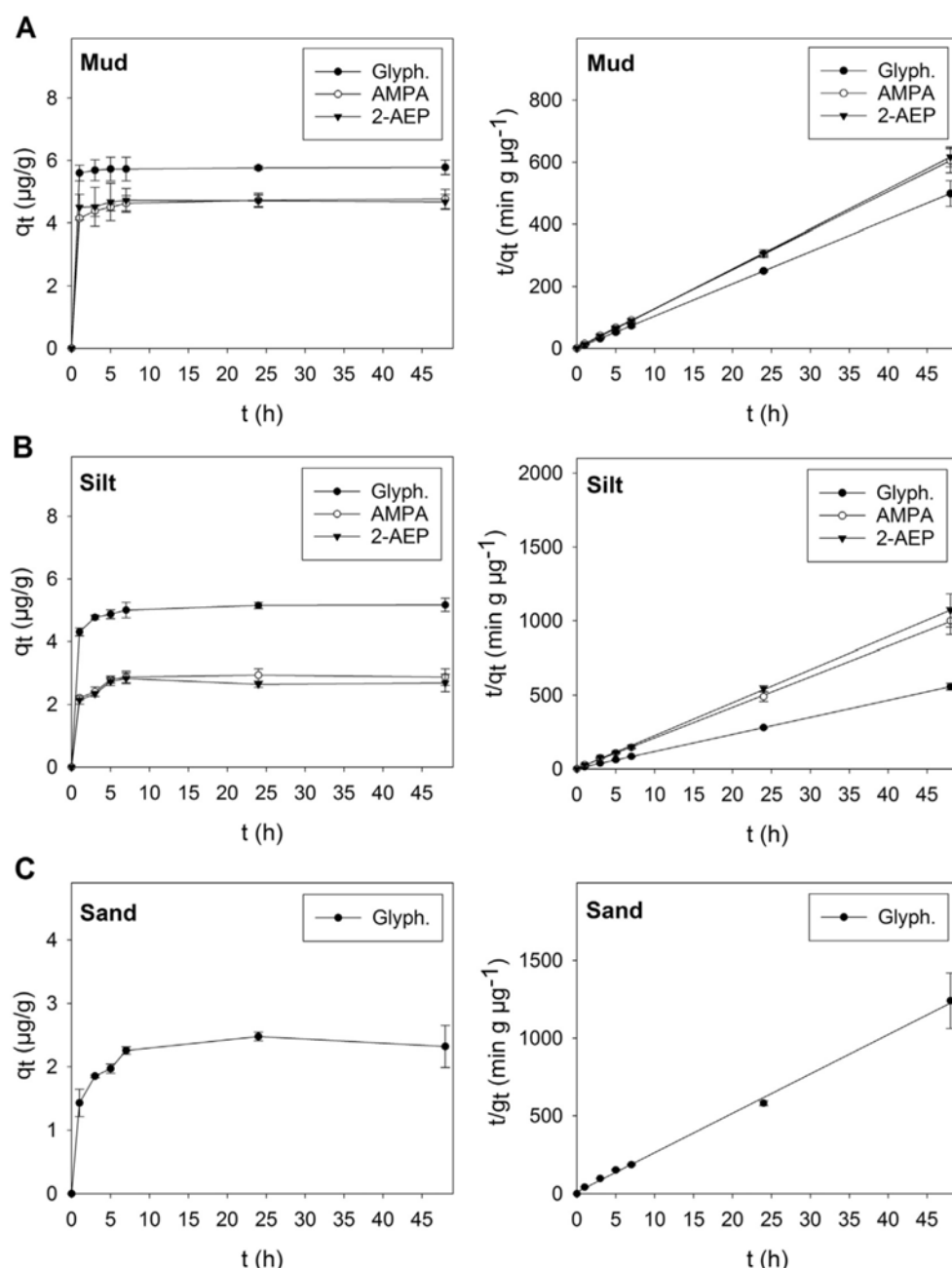


Figure 2. Adsorption equilibrium time (left) of glyphosate, AMPA, and 2-AEP on A. mud, B. silt, and C. sand, and the respective pseudo-second order kinetics (right). The figures in the left column are based on a concentration of 600 μg of each compound/L.

As shown in Figure 2, glyphosate, AMPA, and 2-AEP followed similar adsorption kinetics in the mud and silt sediments, and on sand for glyphosate. The adsorption kinetics consisted of two distinct stages: a fast adsorption process in the first hour followed by slow adsorption. The adsorption equilibrium of glyphosate, AMPA, and 2-AEP was reached in 24 h. The amount adsorbed of glyphosate was higher than those of AMPA and 2-AEP for the three types of sediment. The adsorption rate of glyphosate was the highest on mud, followed by silt and sand (96.3 %, 86.2 %, and 38.6 %, respectively). The adsorption rates of AMPA and 2-AEP on mud and silt were similar (~80 % and ~50 %, respectively). The latter observation can be explained that AMPA and 2-AEP own the same functional groups (i.e. each contains phosphonate and amino group), resulting in their similar interactions with sediments.

Lagergren pseudo-first-order and pseudo-second-order models were employed as kinetic models to investigate the rate-controlling steps involved in the adsorption of glyphosate, AMPA, and 2-AEP onto

sediments. The linearized Lagergren pseudo-first-order [Eq. (2)] and pseudo-second-order [Eq. (3)] equations are as follows:

$$\ln(q_e - q_t) = \ln q_e - k_1 t \quad (2)$$

$$t/q_t = 1/k_2 q_e^2 + t/q_e \quad (3)$$

where q_e and q_t are the amount of phosphonates ($\mu\text{g/g}$) adsorbed onto the marine sediments at equilibrium and time t (min), respectively, and k_1 (min^{-1}) and k_2 ($\text{g}/\mu\text{g min}$) are the equilibrium rate constants of the pseudo-first-order and pseudo-second-order models, respectively. The best-fit model was selected based on the values of the linear regression correlation coefficient (R^2). The pseudo-second-order kinetic model efficiently predicted the kinetic behavior of the three compounds on sediments, based on the high R^2 values (0.9982-0.9999), whereas a poor fit of the data was obtained with the pseudo-first-order kinetic model ($R^2 < 0.85$). The rate constant k_2 , the q_e values, and the corresponding linear regression correlation coefficient (R^2) were calculated from the linear plots of t/q_t vs. t (Figure 2) and are shown in Table 1. The good fit obtained with the pseudo-second-order model suggested chemisorption as the rate-limiting step, presumably between the functional groups of the compounds (i.e., the phosphonate, carboxylate, and amino groups) and the sediment surfaces through the sharing or exchange of electrons. As can be seen from Table 1, the calculated adsorption capacity values ($q_{e,\text{cal}}$) from the second order model are well comparable to the experimental adsorption capacity values ($q_{e,\text{exp}}$). Thus, the adsorption kinetics of the three phosphonates on the sediments is more precisely described by the mechanism of surface site-sorbates reaction of pseudo-second-order model. The adsorption capacity of the three compounds followed the sequence glyphosate > AMPA \geq 2-AEP.

Table 1 Pseudo-second order kinetic parameters for the adsorption of glyphosate, aminomethylphosphonic acid (AMPA), and 2-aminoethylphosphonic acid (2-AEP) onto Baltic Sea mud, silt, and fine-sand sediments under the experimental condition of 600 $\mu\text{g/L}$ initial concentrations, 8 g salt/L, pH = 8.1, temperature = 21 °C.

| Sediment | Pseudo-second-order | | | | |
|-------------|------------------------|--------|---|---|----------------------------------|
| | Equation | R^2 | $q_{e,\text{exp}}$ ($\mu\text{g/g}$) | $q_{e,\text{cal}}$ ($\mu\text{g/g}$) | K_2 (g/ $\mu\text{g min}$) |
| Mud | | | | | |
| Glyphosate | $Y = 0.1730X + 0.4567$ | 0.9999 | 5.7804 | 5.7789 | 0.0655 |
| AMPA | $Y = 0.2093X + 2.4457$ | 0.9999 | 4.7778 | 4.7633 | 0.0179 |
| 2-AEP | $Y = 0.2146X + 1.4743$ | 0.9998 | 4.6772 | 4.6705 | 0.0312 |
| Silt | | | | | |
| Glyphosate | $Y = 0.1879X + 2.3688$ | 0.9999 | 4.6998 | 5.1685 | 0.0157 |
| AMPA | $Y = 0.3371X + 3.6885$ | 0.9997 | 2.9070 | 2.9318 | 0.0308 |
| 2-AEP | $Y = 0.5931X + 6.7319$ | 0.9997 | 2.6925 | 1.6432 | 0.0522 |
| Sand | | | | | |
| Glyphosate | $Y = 0.4218X + 10.449$ | 0.9982 | 2.3708 | 2.8043 | 0.0170 |
| AMPA | NA | NA | NA | NA | NA |
| 2-AEP | NA | NA | NA | NA | NA |

NA: not applicable.

Adsorption isotherms

Linear partitioning and Freundlich models are common adsorption isotherms that were applied in this study to describe the adsorption equilibrium of glyphosate, AMPA, and 2-AEP on marine sediments.

Linear partitioning is described by Eq. (4) and the linear formula of the Freundlich isotherm is shown in Eq. (5):

$$q_e = k_d c_e \quad (4)$$

$$\log q_e = \log k_f + 1/n \log c_e \quad (5)$$

where c_e is the concentration ($\mu\text{g/L}$) in the aqueous phase at equilibrium, and k_d (L/g) the distribution coefficient for the sediment/solution ratio (1/10). The k_d values (Table 2) were obtained from the slope of the linear plots of q_e ($\mu\text{g/g}$) vs. c_e ($\mu\text{g/L}$) (Figure 4). k_f ($\mu\text{g/g}$) is the Freundlich constant (i.e. sorption capacity), and $1/n$ an empirical parameter related to the intensity of adsorption. The values for k_f and $1/n$ (Table 2) were determined from the intercept and slope of the plots $\log q_e$ vs. $\log c_e$ (Figure 4). As shown in Figure 4, both isotherms described the equilibrium adsorption of the three phosphonates on mud and silt. The Freundlich model had a slightly better fit than the linear partitioning model based on the higher R^2 values (0.96 and 0.99), which suggests that the adsorption takes place on heterogeneous surfaces. It is important to point out that the concentrations of the compounds tested in this study of marine sediments were lower than those typically used in soil adsorption studies, as they were considered representative of conditions in the marine ecosystem. Thus, fitting of the data to both models might be a result of the narrow concentration range (120-1200 $\mu\text{g/L}$) tested in this study.

The k_d values obtained from linear partitioning were in the range of 55.2 to -259.5 L/kg for glyphosate, 10.0-39.5 L/kg for AMPA, and 7.7-38.5 L/kg for 2-AEP. Data on glyphosate adsorption in the sandy sediment could only be fitted with the Freundlich model ($R^2 = 0.99$), not with linear partitioning ($R^2 = 0.607$), which suggested adsorption saturation by the sand as the glyphosate concentration increased. The AMPA and 2-AEP concentrations measured in the aqueous phase were relatively stable, indicative of their difficult adsorption onto sand.

In the Freundlich isotherm, higher k_f values represent a larger adsorption capacity. The calculated k_f values for glyphosate, AMPA, and 2-AEP were in the range 129.8-397.7 L/kg , 25.3-73.5 L/kg , and 19.9-70.1 L/kg , respectively. The k_d and k_f values obtained in this study clearly demonstrated the higher adsorption capacity of glyphosate than of the other studied compounds. The parameter $1/n$ represents the linearity of the relationship between C_{aq} and C_{sediment} , with a lower $1/n$ value indicating a less homogeneous distribution of the adsorption site energy on the sediments. For all of the tested compounds, the $1/n$ values were <1 : 0.527-0.917 for glyphosate, 0.784-0.899 for AMPA, and 0.779-0.882 for 2-AEP. The higher $1/n$ value of glyphosate implied that the variability of the sediment adsorption sites had a smaller effect on its adsorption than was the case for AMPA or 2-AEP. The $1/n$ values for the three compounds decreased according to the sequence mud > silt > sand, reflecting the increasingly difficult (i.e., concentration-dependent) adsorption process.

The influence of sediment organic carbon content on the adsorption of glyphosate, AMPA, and 2-AEP was determined by examining their correlations. The sediment organic carbon normalized distribution coefficient (k_{oc}) was calculated from the Freundlich isotherm using Eq. (6). The results are provided in Table 2:

$$K_{oc} = (k_f \times 100)/\text{TOC}\% \quad (6)$$

The k_{oc} values of glyphosate were in the range of 5706-86,540 L/kg , but were higher in the sandy sediment, which had the lowest TOC content (0.15 %). This result demonstrated that sediment organic carbon content is not a determining factor in glyphosate adsorption. For AMPA and 2-AEP, the k_{oc} values decreased with the decreasing TOC content, which suggested that the adsorption of both compounds was more sensitive to the organic carbon content of the sediments than glyphosate. The soil mineral composition, which includes aluminium and iron oxides, is a major factor governing glyphosate and AMPA adsorption. In this study, a positive correlation was also determined between the aluminium and iron contents of the sediments and the adsorption of glyphosate, AMPA, and 2-AEP.

Table 2 Parameters obtained from the linear partitioning and Freundlich adsorption isotherms

of glyphosate, AMPA, and 2-AEP on mud, silt, and sandy sand sediments under the experimental condition of 8 g salt/L, pH =8.1, temperature = 21 °C.

| Sediment | Linear partitioning model | | Freundlich model | | | |
|------------|---------------------------|-------|------------------|-----------------|-------|-------|
| | K_d (L/kg) | R^2 | K_f (L/kg) | K_{oc} (L/kg) | $1/n$ | R^2 |
| Mud | | | | | | |
| Glyphosate | 259.5 | 0.994 | 397.7 | 7152.9 | 0.917 | 0.999 |
| AMPA | 39.5 | 0.992 | 73.5 | 1321.9 | 0.889 | 0.998 |
| 2-AEP | 38.5 | 0.992 | 70.1 | 1259.0 | 0.882 | 0.994 |
| Silt | | | | | | |
| Glyphosate | 55.2 | 0.990 | 141.5 | 5706.1 | 0.849 | 0.999 |
| AMPA | 9.2 | 0.988 | 25.3 | 1019.4 | 0.784 | 0.996 |
| 2-AEP | 7.7 | 0.987 | 19.9 | 802.4 | 0.779 | 0.998 |
| Sand | | | | | | |
| Glyphosate | 6.1 | 0.607 | 129.8 | 86,540.0 | 0.527 | 0.992 |
| AMPA | NA | NA | NA | NA | NA | NA |
| 2-AEP | NA | NA | NA | NA | NA | NA |

NA: not applicable.

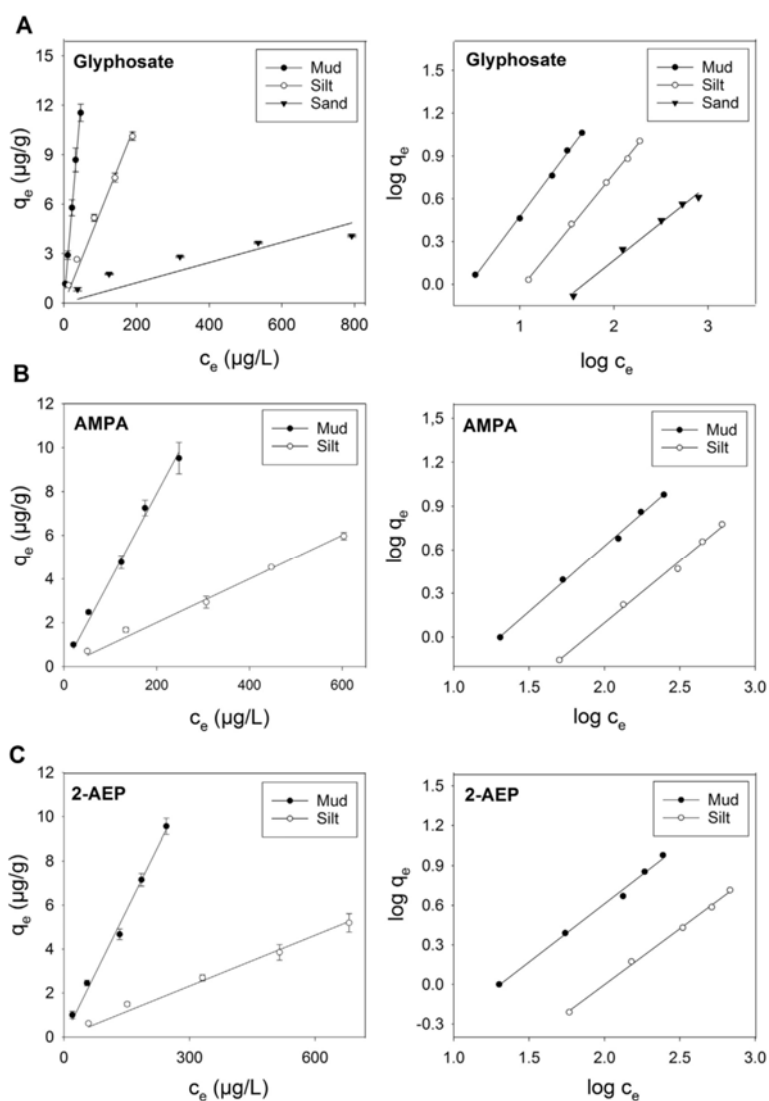


Figure 4. Linear partitioning isotherm (left) and Freundlich isotherm (right) of A. glyphosate, B. AMPA, and C. 2-AEP on marine mud, silt, and sandy sediments.

Effect of environmental factors

The impact of environmental factors, including the pH, salinity, and temperature of the medium, on the adsorption behaviors of glyphosate, AMPA, and 2-AEP was investigated in the mud sediment. The choice of this sediment is due to its greater adsorption capacity for the compounds than silt and sandy sediments. The initial concentrations of the three compounds in the salinity and temperature tests was 300 $\mu\text{g/L}$, and in the pH test 120 $\mu\text{g/L}$.

Effect of the medium pH

To elucidate the effect of the pH of the medium on phosphonate adsorption onto the mud sediment, artificial seawater (a salt concentration of 8 g/L, 0.1 % CHCl_3) was adjusted to three different pH values (7.3, 8.1, 8.7) reflecting the variability of the pH of Baltic Sea water. The pH was adjusted using concentrated HCl and NaOH. The mud sediment samples were incubated for 48 h in the corresponding medium and then spiked with the test compounds. The experiment was then conducted as described for the standard experiment at 21°C. As seen in Figure 5A, adsorption of the three compounds increased significantly ($p < 0.05$) as the pH decreased from 8.7 to 7.3. The results suggested the similar effects of a change in seawater pH on 2-AEP and AMPA. As the pH of the medium increases, the positive surface charge of the sediment decreases and may become negative. Thus, in this study, the decreased adsorption may have been due to the reduced coordination between the phosphonate group of the compounds and the surface of the sediments. In addition, a higher pH may enhance the release of native organic matter from the sediment into solution, thereby reducing the sediment adsorption capacity of the target compounds.

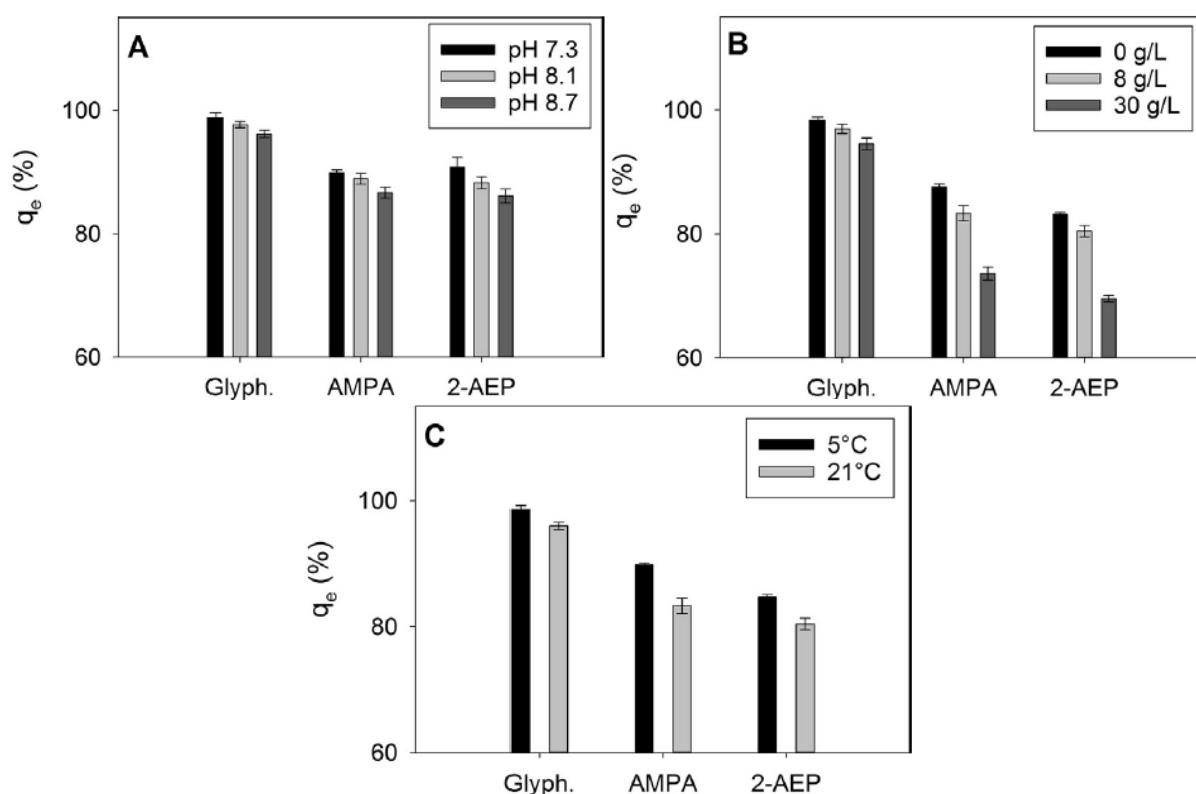


Figure 5. The influence of A. pH, B. salinity, and C. temperature on the adsorption of glyphosate, AMPA, and 2-AEP onto mud sediment. The data are based on duplicate experiments, each consisting of triplicate measurements. The initial concentrations of the compounds were 120 $\mu\text{g/L}$ in the pH experiment and 300 $\mu\text{g/L}$ in the salinity and temperature experiments.

Effect of solution salinity

Salinity (ionic strength) may have an important influence on the adsorption behavior of amphoteric compounds, including glyphosate, AMPA, and 2-AEP, in seawater-sediment systems. To investigate its effect, media containing three different salt concentrations (0, 8, 30 g/L) were prepared. The salt-free

medium (0 g/L) consisted of LC-MS grade water, presumably free of salt. The experiment was run at pH 8.1 and 21°C. The results revealed the negative correlation between the adsorption of the compounds and the salinity of the medium (Figure 5B). The adsorption capacity increased significantly ($p < 0.05$) as the salt concentration decreased from 30 g/L to 0 g/L, an effect attributable to ion exchange. At pH 8.1, glyphosate and AMPA carry negative charges related to the phosphonate (both molecules) and carboxylate (glyphosate) groups and positive charges related to the amino group (both compounds). Most sediment surfaces carry a net negative charge but at pH 8.1 positive charges in sediment organic matter might be exposed. Therefore, changing the ionic composition of the medium may influence the adsorption process, by promoting competition for ion-exchangeable sites. Alternatively, complexes between the phosphonates and cations such as Ca^{2+} and Mg^{2+} , present in the medium, may form that have a lower adsorption affinity for the sediments than do free compounds, such that their adsorption decreases with increasing salinity. According to the results, the various salt concentrations had similar effects on the adsorption behaviors of 2-AEP and AMPA, perhaps because they have the same functional groups.

Effect of temperature

To examine the influence of temperature on the adsorption behaviors of glyphosate, AMPA, and 2-AEP, two different temperatures (5°C and 21°C) were tested. As shown in Figure 5C, the amount of adsorbed compounds increased significantly ($p < 0.05$) as the temperature decreased, indicating that adsorption was an exothermic process. The amount of adsorbed glyphosate, AMPA, and 2-AEP increased differentially as the temperature decreased; at rates of 1.5 %, 6.5 %, and 4.3 %, respectively. This may have been due to the different effects of temperature on the water solubility of the compounds. In general, the solubility of chemical substances improves as the temperature rises, such that the amounts entering the solid phase will be lower when equilibrium is reached. Moreover, an increase in the temperature of the medium could increase the solubility of organic matter in sediments, thus increasing the competition with phosphonates for sediment adsorption.

Environmental implications

Mud sediments can act as a sink for glyphosate as well as for AMPA and 2-AEP, based on the high adsorption affinities of these compounds (>96 % and >78 %, respectively). In silt, the three compounds were distributed between the water and adsorption to the sediment, with a higher tendency of the latter. This result clearly supports the need for bioavailability and toxicity studies of benthic as well as pelagic organisms. Sandy sediments had a weak adsorption capacity for glyphosate, and a negligible adsorption capacity for glufosinate, AMPA, and 2-AEP. Therefore, these compounds can be easily moved from Baltic Sea regions characterized by sandy sediments to those with mud or silt sediments. The pH, salinity, and temperature data demonstrated that the variability of these parameters significantly influences the adsorption behaviors of glyphosate, AMPA, and 2-AEP. A decrease in either the seawater pH or the temperature enhanced the adsorption of these compounds onto marine sediments. Thus, their mobility is a more important factor in warmer than in colder marine systems. Furthermore, the warming effect induced by climate change may influence the fate of phosphonates in the marine environment. The negative correlation between salinity and adsorption suggested the greater mobility of these compounds in marine than in freshwater systems. In the Baltic Sea, salinity varies greatly from south to north, and from east to west, increasing from 2 to 4 in the northern area up to 20-30 in the southwestern area of the sea. Thus, the distribution of glyphosate, AMPA, and 2-AEP in Baltic Sea water and sediments is most likely spatially dependent. These results provide basic information about the fate of these phosphonates in the Baltic Sea and highlight the importance of monitoring these compounds in marine water and sediments, especially in semi-closed seas such as the Baltic Sea, where contaminants may cause acute effects.

Conclusion

In this work, the adsorption of glyphosate, glufosinate, AMPA, and 2-AEP onto mud, silt, and sandy sediments of the Baltic Sea was investigated. Glufosinate had no adsorption affinity for any of the sediments tested. Data on the adsorption kinetics of the other compounds could be well fitted with a second-order rate model. The adsorption rate followed the order glyphosate > AMPA \geq 2-AEP

>glufosinate. Linear partitioning and Freundlich isotherms described the adsorption of glyphosate, AMPA, and 2-AEP on mud and silt. However, only glyphosate showed important adsorption onto the sandy sediment and its behavior could be well modeled with the Freundlich isotherm. The adsorption capacity of the sediments decreased in the order mud >silt >sand. Inverse correlations between the pH, salinity, and temperature of the medium and the adsorption of glyphosate, AMPA, and 2-AEP were determined. This study showed that a small difference in the chemical structure of amphoteric substances such as glyphosate and glufosinate can lead to large differences in their adsorption behaviors.

3. Assessment and conclusion

Assessment and conclusion by applicant:

The study describes the sorption of glyphosate and AMPA to sediments of the Baltic Sea. The described sediments are not relevant for agricultural land use. Some information is missing to check the validity of the experiment (no mass balances, test items not sufficiently described).

The study is therefore classified as reliable with restrictions (Category 2).